

EFFECTIVE FIELD THEORY APPROACH TO PARTON-HADRON CONVERSION IN HIGH ENERGY QCD PROCESSES

K. Geiger

CERN TH-Division, CH-1211 Geneva 23, Switzerland

Abstract

A QCD based effective action is constructed to describe the dynamics of confinement and symmetry breaking in the process of parton-hadron conversion. The deconfined quark and gluon degrees of freedom of the perturbative QCD vacuum are coupled to color singlet collective fields representing the non-perturbative vacuum with broken scale and chiral symmetry. The effective action recovers QCD with its scale and chiral symmetry properties at short space-time distances, but yields at large distances ($r \gtrsim 1$ fm) to the formation of symmetry breaking gluon and quark condensates. The approach is applied to the evolution of a fragmenting $q\bar{q}$ pair with its generated gluon distribution, starting from a large hard scale Q^2 . The modification of the gluon distribution arising from the coupling to the non-perturbative collective field results eventually in a complete condensation of gluons. Color flux tube configurations of the gluons in between the $q\bar{q}$ pair are obtained as solutions of the equations of motion. With reasonable parameter choice, the associated energy per unit length (string tension) comes out $\simeq 1$ GeV/fm, consistent with common estimates.

e-mail: klaus@surya11.cern.ch

CERN-TH. 7440/94, September 1994

1. INTRODUCTION

The physics of QCD exhibits different relevant excitations at different length scales. At space-time short distances (below 1 fm) the relevant degrees of freedom are quarks and gluons whose interactions are well described by perturbative QCD [1, 2]. The long distance physics on the other hand is governed by the hadronic degrees of freedom, and the particles which are observed at large scales are hadrons whose interactions are well described by chiral models [3]. The change of resolution of our microscope with which we probe the physics of QCD is formally described by a renormalization group equation, or evolution equation, that determines the scale dependence of the theory [4, 5, 6].

The transition from short distance (high momentum transfer) regime to the long distance (low energy) domain can be cast in terms of an evolution equation for an *effective QCD action* that embodies *both*, fundamental partonic degrees and hadronic degrees of freedom. By increasing the distance scale (decreasing the momentum scale), the evolution [7] of the effective field theory must lead from one set to the other set of degrees of freedom.

Experiments on high energy QCD processes, such as e^+e^- annihilation, deep inelastic ep scattering, Drell Yan, etc., strongly support the conception that the observed parton fragmentation into hadrons is a universal mechanism. Moreover, the dynamical transformation of color charged quarks and gluons in high energy QCD processes into colorless hadrons is commonly believed to be a local phenomenon [8]. Thus, a consistent description of the local hadronization mechanism must be independent of the details of the partons prehistory and should in principle apply also to hadron-hadron, hadron-nucleus, or nucleus-nucleus collisions.

To date most of the theoretical tools to study properties of QCD are inadequate to describe the dynamics of the transformation from partonic to hadronic degrees of freedom: Perturbative techniques are limited to the deconfined, short distance regime of high energy partons [9], QCD sumrules [10] and effective low energy models [11] are restricted to the long distance domain of hadrons, and lattice QCD [12] lacks the capability of dynamical calculations concerning the quark-gluon to hadron conversion. On the other hand, phenomenological approaches to parton fragmentation [13], are mostly based on hadronization models with adhoc prescriptions to simulate hadron formation from parton decays.

In this paper I follow a rather different, universal approach to the dynamic transition

between partons and hadrons based on an effective QCD field theory description, as recently proposed in Ref. [14]. In the spirit of the aforementioned evolution of effective field theory from high energy to low energy scales [5, 7], the key element is to project out the *relevant degrees of freedom* for each kinematic regime and to embody them in an effective QCD Lagrangian which recovers QCD with its scale and chiral symmetry properties at high momentum transfer, but yields at low energies the formation of symmetry breaking gluon and quark condensates including excitations that represent the physical hadrons. In Sec. 2, I will first formulate the general field theoretical framework. On the basis of the dual vacuum picture of coexisting perturbative and non-perturbative domains an effective action is constructed that embodies the correct scale and symmetry properties of QCD. The concept is here more phenomenologically motivated than the related formal approach of Ref. [7]. However, there appears to be a clear correspondance between those two descriptions. In Sec. 3, I shall demonstrate the applicability of this effective QCD field theory to the dynamics of parton-hadron conversion by exemplarily considering the evolution of gluons produced by a fragmenting quark-antiquark pair. The change of the gluon distribution in the presence of a confining composite field is studied and flux tube solutions of the gluon field resulting from the equations of motion are analyzed in terms of the string tension, that characterizes the effective confinement potential. Various perspectives of the approach are discussed in Sec. 4, in particular the applicability to the QCD phase transition, and high density QCD.

2. EFFECTIVE QCD FIELD THEORY WITH SPONTANEOUS SYMMETRY BREAKING

The goal is to construct an effective field theory that describes the dynamics of *both* partonic and hadronic degrees of freedom and their interplay. The approach is based on the concept of the effective action [4, 7], which will be represented here as ($r \equiv r^\mu$ denotes the space-time 4-vector)

$$S_{eff} = \int d^4r \left[\mathcal{L}[\psi, \mathcal{A}] + \mathcal{L}[\chi, \mathcal{U}] + \mathcal{L}[\psi, \mathcal{A}, \chi] \right] . \quad (1)$$

The three contributions to the action, which will be discussed below, correspond to the QCD Lagrangian with the quark (ψ_i) and gluon fields (A_a), an effective low energy Lagrangian introducing composite fields χ and U , and a term that couples the "microscopic"

fundamental quark and gluon degrees of freedom to the "macroscopic" fields χ and U which represent the hadronic degrees of freedom.

2.1 $\mathcal{L}[\psi, \mathcal{A}]$

The QCD Lagrangian in (1) contains the gluon fields A_a^μ coupled to massless quark fields ψ_i ($i = 1, \dots, N_f$),

$$\mathcal{L}[\psi, \mathcal{A}] = -\frac{\infty}{\Delta} \mathcal{F}_{\mu\nu, \mp} \mathcal{F}_\mp^{\mu\nu} + \bar{\psi}_\gamma \left[\gamma_\mu \partial^\mu - \int_f \gamma_\mu \mathcal{A}_\mp^\mu \mathcal{T}_\mp \right] \psi_\gamma + \mathcal{L}_{\int \square} + \mathcal{L}_{\int \square}. \quad (2)$$

Here $F_a^{\mu\nu} = \partial^\mu A_a^\nu - \partial^\nu A_a^\mu + g_s f_{abc} A_b^\mu A_c^\nu$ is the gluon field strength tensor. The subscripts a, b, c label the color components and g_s denotes the color charge related to $\alpha_s = g_s^2/(4\pi)$. The T_a are the generators of the $SU(3)$ color group, satisfying $[T_a, T_b] = i f_{abc} T_c$ with the structure constants f_{abc} . The gauge fixing term $\mathcal{L}_{\int \square} = \infty / (\in \mp) (\eta_\mu \mathcal{A}_\mp^\mu)^\infty$ with gauge parameters a and η_μ , and the contribution of Fadeev-Popov ghost fields ζ , $\mathcal{L}_{\int \square} = (\partial_\mu \zeta^*) (\delta_\mp \partial^\mu - \int_f \{ \square \} \mathcal{A}_\mp^\mu) \zeta_\mp$, will be irrelevant later on, because a physical gauge $\eta \cdot A = 0$ can be fixed, which eliminates the presence of ghosts.

The Lagrangian (2) is well known to be invariant under chiral transformations [3]. At the tree level it is also invariant under scale transformations $r_\mu \rightarrow r'_\mu = e^\Delta r_\mu$ [15], generated by a so-called dilaton charge $D(t) = \int d^3r J_0^S(r)$, where J_μ^S is the scale current and $[D, \varphi(r)] = i(r_\mu \partial^\mu + d_\varphi) \varphi(r)$ for a generic quantum field φ with scale dimension d_φ . The convention is $d_A = 1$ for gauge boson fields and $d_\psi = 3/2$ for fermion fields. It follows that $\mathcal{L}(\psi, \mathcal{A})$ has scale dimension 4 so that $[D, \mathcal{L}(\psi, \mathcal{A})] = 0$ and therefore massless QCD proves to be scale invariant at tree level.

At high energies and short space-time distances, asymptotic freedom leads to unconfined gluon and quark fields in (2). However, in the physical world these color degrees of freedom are confined, and both chiral and scale symmetry are explicitly broken. To describe the dynamics of the symmetry breakdown of the transition between the perturbative, scale and chiral invariant, regime and the non-perturbative world with broken symmetries, one needs to supplement (2) (by adding $\Delta\mathcal{L} = \mathcal{L}[\chi, \mathcal{U}] + \mathcal{L}[\psi, \mathcal{A}, \chi]$) to construct an effective description such that at high energies the fully symmetric QCD phase is recovered, but at low energies massive hadrons emerge.

2.2 $\mathcal{L}[\chi, \mathcal{U}]$

The specific form of $\mathcal{L}[\chi, \mathcal{U}]$ in (1) is adopted from Refs. [16, 17], where an effective low energy Lagrangian was constructed, guided by the scale and chiral symmetry properties of the QCD Lagrangian. The construction is based on the observation that even massless QCD is no longer scale invariant when going beyond tree level, because of the scale anomaly [15] $\partial^\mu J_\mu^S = \beta(g_s)/(2g_s)F_{\mu\nu}F^{\mu\nu}$, where J_μ^S is the scale current as before. In addition chiral invariance breaks down when finite quark masses are taken into account. As a consequence, the QCD energy momentum tensor $\theta_{\mu\nu}$ exhibits the well known *trace anomaly* [18]:

$$\theta_\mu^\mu = \frac{\beta(\alpha_s)}{4\alpha_s} F_{\mu\nu}F^{\mu\nu} + (1 + \gamma_m) \sum_q m_q \bar{q}q, \quad (3)$$

where β is the Callan-Symanzik function and γ_m is the anomalous mass dimension. This anomaly constrains the form of the effective low energy Lagrangian, because without it Poincaré invariance would be broken, and the mass of the proton would come out wrong, since $2m_p^2 = \langle p|\theta_\mu^\mu|p\rangle$.

The extension of these symmetry properties of the QCD Lagrangian to the low energy domain was modeled by Campbell, Ellis and Olive [17] as¹

$$\begin{aligned} \mathcal{L}[\chi, \mathcal{U}] = & \frac{1}{2} (\partial_\mu \chi)(\partial^\mu \chi) + \frac{1}{4} Tr \left[(\partial_\mu U)(\partial^\mu U^\dagger) \right] - b \left[\frac{1}{4} \chi_0^4 + \chi^4 \ln \left(\frac{\chi}{e^{1/4} \chi_0} \right) \right] \\ & - c Tr \left[m_q (U + U^\dagger) \right] \left(\frac{\chi}{\chi_0} \right)^3 - \frac{1}{2} m_0^2 \phi_0^2 \left(\frac{\chi}{\chi_0} \right)^4. \end{aligned} \quad (4)$$

This form introduces a *scalar gluon condensate field* χ and a *pseudoscalar quark condensate field* $U = f_\pi \exp \left(i \sum_{j=0}^8 \lambda_j \phi_j / f_\pi \right)$ for the nonet of the meson fields ϕ_j ($f_\pi = 93$ MeV, $Tr[\lambda_i \lambda_j] = 2\delta_{ij}$, $UU^\dagger = f_\pi^2$), with non-vanishing vacuum expectation values

$$\chi_0 = \langle 0 | \chi | 0 \rangle \neq 0, \quad U_0 = c \langle 0 | U + U^\dagger | 0 \rangle \neq 0 \quad (5)$$

that explicitly break scale, respectively chiral symmetry. In (4), b is related to the conventional bag constant B by $B = b\chi_0^4/4$, c is a constant of mass dimension 3, $m_q = \text{diag}(m_u, m_d, m_s)$ is the light quark mass matrix, and m_0^2 is an extra U(1)-breaking mass term for the ninth pseudoscalar meson ϕ_0 .

¹In Ref. [17] the second term in eq. (4) was scaled by a factor $(\chi/\chi_0)^2$, which however is not necessary [16], since just this term gives a chiral symmetric contribution in agreement with the QCD anomaly (3).

Notice that the anomaly constraint (3) is modeled by the third and fourth term in (4) with the correspondence

$$\langle 0 | \frac{\beta(\alpha_s)}{4\alpha_s} F_{\mu\nu} F^{\mu\nu} | 0 \rangle = -b \chi_0^4 \quad (6)$$

and

$$\langle 0 | \bar{q}q | 0 \rangle = c \left(\frac{\chi}{\chi_0} \right)^3 \langle 0 | U + U^\dagger | 0 \rangle . \quad (7)$$

2.3 $\mathcal{L}[\psi, \mathcal{A}, \chi]$

The key ingredient in (1) is the connection between the scale and chiral symmetric, short distance regime of colored fluctuations and the world of colorless hadrons with broken symmetries. It is mediated by the coupling between the fundamental quark and gluon degrees and the collective fields χ and U through coupling functions $g(\chi)$ and $\xi(\chi)$,

$$\mathcal{L}[\psi, \mathcal{A}, \chi] = \frac{\xi(\chi)}{\Delta} \mathcal{F}_{\mu\nu, +} \mathcal{F}_+^{\mu\nu} - \bar{\psi} \psi \}(\chi) \psi . \quad (8)$$

The coupling functions $\xi(\chi)$ and $g(\chi)$ are chosen in the spirit of Friedberg and Lee [19], who formulated a *dual QCD vacuum picture*: High momentum, short distance quark-gluon fluctuations (the perturbative vacuum) are embedded in a collective background field χ (the non-perturbative vacuum), in which by definition the low momentum, long range fluctuations are absorbed. Confinement is thus associated with the colordielectric structure of the QCD vacuum. This property is modeled by a colordielectric function

$$\kappa(\chi) = 1 - \xi(\chi) \quad (9)$$

that satisfies

$$\kappa(0) = 1 , \quad \kappa(\chi_0) = 0 , \quad (10)$$

thereby generating color charge confinement, because a color electric charge creates a displacement $\vec{D}_a = \kappa \vec{E}_a$, where $E_a^k = F_a^{0k}$, with energy $\frac{1}{2} \int d^3r D_a^2 / \kappa$ which is infinite for non-zero total charge if κ falls off faster than $1/\sqrt{r}$ for large distances r . The particular form of $\kappa(\chi)$ is not crucial as long as the properties (10) are satisfied [20]. A specific choice is [21]

$$\kappa(\chi) = 1 + \left(\frac{\chi}{\chi_0} \right)^3 \left(3 \frac{\chi}{\chi_0} - 4 \right) \theta(\chi) , \quad (11)$$

which has the further properties of $\kappa'(0) = \kappa''(0) = 0$. Other forms used in the literature are e.g. $\kappa(\chi) = |1 - (\chi/\chi_0)^n|^m$ [22] (Friedberg and Lee originally proposed $n = m = 1$).

Similarly, absolute confinement can be ensured also for quarks by coupling the quark fields to the χ -field through [23]

$$g(\chi) = g_0 \left(\frac{1}{\kappa(\chi)} - 1 \right), \quad (12)$$

which leads to an effective confinement potential with the masses of the quarks inside approximately equal to the current masses, but at $\chi = \chi_0$ it generates an infinite asymptotic quark mass (the value of g_0 is irrelevant in the present paper).

2.4 Equations of motions

To summarize to this end, the complete effective action (1) is determined by the Lagrangian

$$\begin{aligned} \mathcal{L}_{\{\psi, \mathcal{A}\}} &= \mathcal{L}[\psi, \mathcal{A}] + \mathcal{L}[\chi, \mathcal{U}] + \mathcal{L}[\psi, \mathcal{A}, \chi] \\ &= -\frac{1}{4} \kappa(\chi) F_{\mu\nu, a} F_a^{\mu\nu} + \bar{\psi}_i \left[i\gamma_\mu \partial^\mu - g_s \gamma_\mu A_a^\mu T_a - g(\chi) \right] \psi_i \\ &\quad + \frac{1}{2} (\partial_\mu \chi)(\partial^\mu \chi) + \frac{1}{4} \text{Tr} \left[(\partial_\mu U)(\partial^\mu U^\dagger) \right] - V(\chi, U), \end{aligned} \quad (13)$$

plus the terms $\mathcal{L}_{\{\mathcal{A}, \mathcal{U}\}}$ and $\mathcal{L}_{\{\chi, U\}}$ of (2). The potential V is given by

$$\begin{aligned} V(\chi, U) &= b \left[\frac{1}{4} \chi_0^4 + \chi^4 \ln \left(\frac{\chi}{e^{1/4} \chi_0} \right) \right] \\ &\quad + c \text{Tr} \left[\hat{m}_q (U + U^\dagger) \right] \left(\frac{\chi}{\chi_0} \right)^3 + \frac{1}{2} m_0^2 \phi_0^2 \left(\frac{\chi}{\chi_0} \right)^4, \end{aligned} \quad (14)$$

which has its minimum when $\chi = \chi_0 = \langle 0|\chi|0 \rangle$ and equals the vacuum pressure (bag constant) $B = b\chi_0^4/4$ at $\chi = 0$. Typical forms of $V(\chi, U)$ for different values of B and m_q are depicted in Fig. 1.

The effective field theory defined by (1) and (13) represents a description of the duality of partonic and hadronic degrees of freedom by coupling the high energy QCD phase with unconfined gluon and quark degrees of freedom to a low energy QCD phase with confinement and broken chiral symmetry which contains a gluon condensate (6) and a quark-antiquark condensate (7). Small oscillations about the minimum of the potential $V(\chi, U)$ are to be interpreted as physical hadronic states that emerge after symmetry breaking. They include [17]: (i) glueballs and hybrids as quantum fluctuations in the gluon condensate χ_0 , (ii)

pseudoscalar mesons as excitations of the quark condensate U_0 , (iii) the pseudoscalar flavor singlet meson ϕ_0 , and (iv) baryons as non-topological solitons [24].

The field equations which derive from (1) and (13) are:

$$[\gamma_\mu (i\partial^\mu - g_s A_a^\mu T_a) - g(\chi)] \psi_i = 0 \quad (15)$$

$$\partial_\mu [\kappa(\chi) F_a^{\mu\nu}] = -g_s \kappa(\chi) f_{abc} A_{\mu,b} F_c^{\mu\nu} + g_s \bar{\psi}_i \gamma^\nu T_a \psi_i \quad (16)$$

$$\partial_\mu \partial^\mu \chi + \frac{\partial V(\chi, U)}{\partial \chi} + \frac{\partial \kappa(\chi)}{\partial \chi} F_{\mu\nu,a} F_a^{\mu\nu} + g(\chi) \bar{\psi}_i \psi_i = 0 \quad (17)$$

$$\partial_\mu \partial^\mu U + \frac{\partial V(\chi, U)}{\partial U} = 0. \quad (18)$$

Notice that the U -field does not couple directly to the quark and gluon fields. Per construction [17], the dynamics of the quark condensate field U is solely driven by the gluon condensate field χ . It is important to realize that the interplay between the χ -field and the quark and gluon fields, ψ and A , is the crucial element of this approach.

2.5 Comments

The following remarks concerning the effective Lagrangian (13) are important:

- a) At short distances or high momentum transfers the exact QCD Lagrangian (2) is recovered, since $\chi = U = 0$ and $\kappa(\chi) = 1$ (i.e. $\xi(\chi) = 0$) and $g(\chi) = 0$, whereas the long distance QCD properties emerge as $\chi/\chi_0 \rightarrow 1$ and $U/U_0 \rightarrow 1$ [17] and no colored quanta survive. The transition from one set of degrees of freedom (ψ, A) to the other (χ, U) corresponds to consecutively integrating out all colored quantum fluctuations and absorbing them effectively in the collective color singlet fields.
- b) The problem of double counting degrees of freedom has to be carefully inspected. Although it does not arise in one-loop calculations (to which I will restrict here), processes with e.g. two-gluon exchange could also be contained in the exchange of a color singlet χ -quantum. A minimal possibility to avoid this problem is a rigid separation of high and low momentum modes, by introducing a characteristic scale Q_0 : above Q_0 the physics is described in terms of quark gluon degrees and below Q_0 the dynamics is governed by the collective degrees of freedom [7].
- c) $\mathcal{L}[\chi, \mathcal{U}]$ for the composite fields embodies the correct QCD scaling and chiral properties and accounts for the important anomaly (3) of the physical energy-momentum tensor

of QCD. The coupling between quarks and gluons to the composite field χ in $\mathcal{L}[\psi, \mathcal{A}, \chi]$ can be interpreted in analogy to a thermodynamic system in equilibrium with a heat bath, with a net flow of energy between the system and the heat bath environment such that the *bare* energy of the system is not conserved. However the *free* energy of the system, here high momentum quarks and gluons, is constant [25]. It corresponds to the conserved energy momentum tensor $\theta_{\mu\nu}$ with its non-zero trace (3).

- d) There is no need for explicit renormalization of $\Delta\mathcal{L} = \mathcal{L}[\chi, \mathcal{U}] + \mathcal{L}[\psi, \mathcal{A}, \chi]$. The composite fields χ and U are already interpreted as effective degrees of freedom with loop corrections implicitly included in $\Delta\mathcal{L}$ and it would be double counting to add them again. Moreover, in the present approach the low energy domain of $\mathcal{L}[\chi, \mathcal{U}]$ is per construction bounded from above by the onset of the high energy regime described by $\mathcal{L}[\psi, \mathcal{A}]$. In correspondance to item b) the scale Q_0 that separates the two domains, provides an "ultra-violet" cut-off for $\mathcal{L}[\chi, \mathcal{U}]$, and at the same time an infra-red cut-off for $\mathcal{L}[\psi, \mathcal{A}]$.

This effective field theory approach offers a wide range of physical applications and can be extended and refined in various directions, as discussed in Sec. 4. The scope of the remainder of this paper is however conceived as a exemplary demonstration of how of the dynamics of parton-hadron conversion emerges within this framework.

3. CONFINEMENT OF GLUONS IN A FRAGMENTING $q\bar{q}$ SYSTEM

The effective QCD field theory defined by (13) is readily applicable to describe the dynamic evolution from perturbative to non-perturbative vacuum in high energy processes. In accord with the symmetry breaking formalism of Sec. 2, the parton-hadron transition can be visualized as the conversion of high momentum colored quanta of the fundamental quark and gluon fields into color neutral composite states that are described by the condensate fields χ and U and their excitations.

In the following I shall consider as an example the fragmentation of a $q\bar{q}$ jet system with its emitted bremsstrahlung gluons and describe the evolution of the system as it converts from the parton phase to the hadronic phase. The process is illustrated in Fig. 2: A time-like virtual photon in an e^+e^- annihilation event with large invariant mass $Q^2 \gg \Lambda^2$

is assumed to produce a $q\bar{q}$ pair which initiates a cascade of sequential gluon emissions. (Here and in the following Λ denotes the fundamental QCD scale). The early stage is characterized by emission of "hot" gluons far off mass shell in the perturbative vacuum. Subsequent gluon branchings yield "cooler" gluons with successively smaller virtualities, until they are within Q_0^2 , where Q_0 is of the order of $m_\chi \equiv 4b\chi_0^2 \simeq 1$ GeV. At this point condensation sets in, or loosely speaking, the "cool" gluons are eaten up by the color neutral gluon condensate field χ , the particle excitations of which must then decay into physical hadrons by means of some local interaction in the non-perturbative vacuum. A similar picture holds for the U -field.

It is well known that the bulk of produced particles stems from rather soft gluon emissions that are characterized by small values x of the fraction of the initial energy. Secondary production of $q\bar{q}$ pairs is comparably rare on the perturbative level. It is therefore reasonable to neglect the quark degrees of freedom and study the purely gluonic sector. Furthermore it is convenient to work in a physical (axial) gauge for the gluon fields, $\eta \cdot A = 0$, by choosing the gauge vector in (2) as $\eta_\mu = n_\mu$ with n being space-like and constant, in which case the ghost contribution vanishes. Consequently, the equations of motion (15)-(18) reduce to:

$$\partial_\mu [\kappa(\chi) F_a^{\mu\nu}] = -g_s \kappa(\chi) f_{abc} A_{\mu,b} F_c^{\mu\nu} \quad (19)$$

$$\partial_\mu \partial^\mu \chi = -\frac{\partial V(\chi)}{\partial \chi} - \frac{\partial \kappa(\chi)}{\partial \chi} F_{\mu\nu,a} F_a^{\mu\nu} \quad (20)$$

$$\partial_\mu \partial^\mu U = -4c \left(\frac{\chi}{\chi_0} \right)^3 \text{Tr}[m_q]. \quad (21)$$

The solution of these equations is a still formidable task, because not only the gluon fields but also χ and U are quantum operators. To make progress, I will now proceed by (i) treating the quantum gluon fields perturbatively, and (ii) employing the mean field approximation for the composite fields χ and U . Representing

$$\chi(r) = \bar{\chi}(r) + \hat{\chi}(r), \quad (22)$$

where $\bar{\chi}$ is a c-number and $\hat{\chi}$ a quantum operator (similarly for U), the mean field approximation is obtained by neglecting the quantum fluctuations $\hat{\chi}$ and keeping only $\bar{\chi}$. Thus, the approximations (i) and (ii) correspond to the semiclassical limit in which gluonic quantum fluctuations interact with a classical mean field. To a good approximation this should provide a reasonable description: first, because renormalization group improved QCD perturbation theory allows for an accurate description of the evolution of the gluon field [26] at

short distances where $\chi = 0$, and second, because the dynamics of the system around $\chi = \bar{\chi}$ is governed by a large number of virtual excitations, corresponding to coherent modes of field quanta, so that a quasiclassical mean field description should be applicable in the low energy regime [19].

3.1 Evolution of the gluon distribution in the presence of the collective field χ

As I will show now, the equations of motion (19)-(21) simplify to a perturbative evolution equation for the gluon distribution which is coupled to the equation for the mean field $\bar{\chi}$. The key problem is the first equation, since the gluon fields A^μ , or equivalently $F^{\mu\nu}$, drive the dynamics of the χ -field which in turn feeds back via $\kappa(\chi)$. As mentioned before, the U -field does not couple directly to the gluon field. The procedure in the following is therefore to 'solve' eq. (19) as a function of κ and then to insert the solution into (20), so that one is left (aside from the simple third equation) with a single equation for χ , which however is non-linear.

Solving the equation of motion (19) for the gluon field is equivalent to the calculation of the complete Greens function with an arbitrary number of gluons. Instead, I will restrict to evaluate the 2-point Greens function only (Fig. 3), i.e. the full gluon propagator which includes both the one-loop order gluon self-interaction through real and virtual emission and absorption, and the effective interaction with the confining background field χ . In the framework of "jet calculus" [27], this gluon propagator denoted as $D_g(x, k^2; x_0, Q^2)$, describes how a gluon, produced with an invariant mass Q^2 , evolves in the variable x (momentum or energy fraction) and the virtuality k^2 (or transverse momentum k_\perp^2) through these interactions. To one-loop order, it is obtained by calculating the corresponding cut diagrams. In the present case, one has in addition to the usual gluon branching and fusion processes, $g \rightarrow gg$ and $gg \rightarrow g$, contributions from energy transfer and two gluon annihilation processes $g \rightarrow g\chi$ and $gg \rightarrow \chi$, respectively ². This is illustrated in Fig. 3.

To write down the determining equation for the gluon propagator D_g , it is convenient

²In the present case of $q\bar{q}$ jet evolution, the contribution of perturbative 2-gluon fusion processes $gg \rightarrow g$ for $k^2 \gg \Lambda^2$ is very small [28], but the non-perturbative gluon recombination $gg \rightarrow \chi$ in the range $Q_0^2 \gtrsim k^2 \geq \Lambda^2$ is of essential importance in order to achieve complete confinement.

employ lightcone variables, defined by the identification of components of four-vectors as

$$k^\mu = (k^+, k^-, \vec{k}_\perp) ; \quad k^\pm = \frac{1}{\sqrt{2}}(k^0 \pm k^3) ; \quad k^\perp = (k^1, k^2) . \quad (23)$$

The k^+ component of a particle's momentum, the *light cone momentum*, is always positive definite, $k^+ > 0$, and the *light cone energy*, $k^- = (k_\perp^2 + m^2)/(2k^+)$ is also positive. Furthermore, the *light cone time* $r^+ = (t + z)/\sqrt{2}$ is conjugate to k^- and the *light cone coordinate* r^- is conjugate to k^+ . The invariant momentum space element is

$$\frac{d^3k}{(2\pi)^3 2E} = \frac{d^4k}{(2\pi)^4} \delta^+(k^2 - m^2) = \frac{dk^+ d^2k_\perp}{16\pi^3 k^+} . \quad (24)$$

Choosing the *light cone gauge* for the gluon fields, $\eta \cdot A = A^+ = -A^- = 0$, results in well known simplifications in the perturbative analysis of light cone dominated processes and has the advantage that there are neither negative norm gluon states nor ghost states present [29]. As a consequence only the transverse components A_\perp^i ($i = 1, 2$) are dynamical field variables, since A^+ is identically zero and A^- is determined at any 'time' r^+ by A_\perp^1 and A_\perp^2 . The particular choice $\eta = (p_q + p_{\bar{q}})/2$ has the advantage that interference terms do not contribute [2] to leading log accuracy (they are suppressed $\propto 1/k^2$). Therefore, in the leading log approximation (LLA) [30, 9, 26, 31], it is enough to realize that for every choice of b (Fig. 3 top), one can group the other gluons in a unique way to groups forming dressed rungs of a ladder (Fig. 3 middle) whose discontinuity is taken (Fig. 3 bottom).

Introducing the variable $x = k^+/P^+$ (the light cone fraction), and parametrizing the momenta of initial quark and antiquark as $P \equiv p_q + p_{\bar{q}}$ with

$$P^+ = Q, \quad P^- = \frac{4m_q^2}{2P^+}, \quad \vec{P}_\perp = \vec{0}, \quad (25)$$

i.e. $P^2 = Q^2$, where as before Q denotes the invariant mass of the time-like photon that creates the pair, the determining equation for the gluon propagator $D_g(x, x_0; k^2, Q^2)$ can now be represented in the form (c.f. Appendix A):

$$\begin{aligned} D_g(x, k^2; x_0, Q^2) &= x_0 \delta(x - x_0) \delta(k^2 - Q^2) F_g(Q^2, Q_0^2) \\ &+ F_g(Q^2, k^2) \int_{Q_0^2}^{k^2} \frac{dk'^2}{k'^2} \int_x^1 \frac{dx'}{x'} w(x', x, k^2) D_g(x', k'^2; x_0, Q^2) F_g(k'^2, Q_0^2) \end{aligned} \quad (26)$$

This equation has a simple physical significance: The first term is the inclusive sum of virtual emissions and reabsorptions, and therefore does not change the number of gluons in

the gluonic wavefunction of the fragmenting $Q\bar{Q}$ pair, whereas the second term describes the change of the gluon distribution as a result of real decay or fusion processes. The *Sudakov formfactor*

$$F_g(Q^2, k^2) = \exp \left[- \int_{k^2}^{Q^2} \frac{dk'^2}{k'^2} w_g(k'^2) \right] \quad (27)$$

is the probability a gluon propagates like a bare, non-interacting particle while degrading its virtuality from Q^2 to k^2 . As the gap between Q^2 and k^2 grows, such a fluctuation becomes increasingly unlikely. The *total interaction probability*

$$w_g(k^2) = \int_0^1 dx \int_x^1 \frac{dx'}{x'} w(x', x, k^2) \quad (28)$$

is the integral over the inclusive probability for all possible gluon interaction processes i ,

$$w(x', x, k^2) = \sum_{\text{proceses } i} w_{(i)}(x', x, k^2). \quad (29)$$

The normalization is such that

$$1 = F_g(Q^2, Q_0^2) + F_g(Q^2, k^2) \int_{Q_0^2}^{Q^2} \frac{dk'^2}{k'^2} w_g(k'^2) F_g(k'^2, Q_0^2) \quad (30)$$

in accord with unitarity (probability) conservation. Multiplying (26) by F_g^{-1} , differentiating, and accounting for (30), yields:

$$k^2 \frac{\partial}{\partial k^2} D_g(x, k^2; x_0, Q^2) = \int_x^1 \frac{dx'}{x'} w(x', x, k^2) D_g(x', k^2; x_0, Q^2) - w_g(k^2) D_g(x, k^2; x_0, Q^2) \quad (31)$$

As summarized in the Appendices, one obtains for the individual interaction probabilities $w_{(i)}$ to one loop order (with the assignment $x_1 \rightarrow x_2, (x_1 - x_2)$ for branchings and $x_1, (x_2 - x_1) \rightarrow x_2$ for fusions)

$$\begin{aligned} w_{g \rightarrow gg}(x_1, x_2, k^2) &= \frac{\alpha_s(k^2)}{2\pi} \gamma_{g \rightarrow gg} \left(\frac{x_2}{x_1} \right) \\ w_{g \rightarrow gg}(x_1, x_2, k^2) &= \frac{\alpha_s(k^2)}{2\pi} \left[\frac{8\pi^2 c_{gg \rightarrow g}}{k^2 \Lambda^2} \frac{x_1(x_2 - x_1)}{x_2^2} \right] \gamma_{g \rightarrow gg} \left(\frac{x_1}{x_2} \right) \\ w_{g \rightarrow g\chi}(x_1, x_2, k^2) &= \frac{\lambda_\chi(k^2)}{2\pi} \gamma_{g \rightarrow g\chi} \left(\frac{x_2}{x_1} \right) \\ w_{gg \rightarrow \chi}(x_1, x_2, k^2) &= \frac{\lambda_\chi(k^2)}{2\pi} \left[\frac{8\pi^2 c_{gg \rightarrow \chi}}{k^2 \Lambda^2} \frac{x_1(x_2 - x_1)}{x_2^2} \right] \gamma_{\chi \rightarrow gg} \left(\frac{x_1}{x_2} \right), \end{aligned} \quad (32)$$

where $c_{gg \rightarrow g} = c_{gg \rightarrow \chi} = 1/8$, and

$$\gamma_{g \rightarrow gg}(z) = 2C_A \left(z(1-z) + \frac{z}{1-z} + \frac{1-z}{z} \right)$$

$$\begin{aligned}
\gamma_{g \rightarrow g\chi}(z) &= \frac{1}{4} \left(\frac{1+z^2}{1-z} \right) \\
\gamma_{\chi \rightarrow gg}(z) &= 8 \left(z^2 - z + \frac{1}{2} \right).
\end{aligned} \tag{33}$$

Here $C_A = N_c = 3$, and z is the fraction of x -values of daughter to mother gluons. In (32),

$$\alpha_s(k^2) = \left[b \ln \left(\frac{k^2}{\Lambda^2} \right) \right]^{-1}, \quad b = \frac{11N_c - 2N_f}{12\pi}, \tag{34}$$

is the one loop order QCD running coupling (in the present case $N_f = 0$), and

$$\lambda_\chi(k^2) = \frac{\tilde{\xi}_\chi^2(k^2)}{4\pi} \tag{35}$$

denotes the coupling to the χ -field in momentum space, with $\tilde{\xi}_\chi$ denoting the Fourier transform of $\xi(\chi)$ in (8).

Eq. (26) for the propagator $D_g(x, k^2; x_0, Q^2)$ corresponds the evolution equation for the gluon distribution $g(x, k_\perp^2)$, which is defined [32] as average number of gluons at 'light cone time' $r^+ = 0$ in the multi-gluon state³ $|P\rangle$ with light cone fractions $x \equiv k^+/P^+$ in a range dx and transverse momenta in a range d^2k_\perp :

$$x g(x, k_\perp^2) = \frac{1}{P^+} \int \frac{dr^- d^2r_\perp}{(2\pi)^3} e^{-i(k^+r^- - \vec{k}_\perp \cdot \vec{r}_\perp)} \langle P | F_a^{+\mu}(0, r^-, \vec{r}_\perp) F_{a,\mu}^+(0, 0, \vec{0}_\perp) | P \rangle \tag{36}$$

Thus, as is evident from Fig. 3, the probability for finding a gluon with x and k_\perp^2 is given by the identification

$$g(x, k_\perp^2) = D_g(x, k^2; 1, Q^2) \Big|_{k^2=k_\perp^2}. \tag{37}$$

On account of the explicit expressions (32)-(35), and taking as evolution variable the gluon transverse momentum k_\perp^2 rather than the invariant mass k^2 [33], one finally arrives at the master equation for the evolution of the gluon distribution:

$$\begin{aligned}
k_\perp^2 \frac{\partial}{\partial k_\perp^2} g(x, k_\perp^2) &= + \frac{\alpha_s(k_\perp^2)}{2\pi} \int_0^1 dz \left[\frac{1}{z} g\left(\frac{x}{z}, k_\perp^2\right) - \frac{1}{2} g(x, k_\perp^2) \right] \gamma_{g \rightarrow gg}(z) \theta(k_\perp^2 - Q_0^2) \\
&\quad - \frac{\alpha_s(k_\perp^2)}{2\pi} \left(\frac{\Lambda^2}{k_\perp^2} \right) 8\pi^2 c_{gg \rightarrow g} \int_0^1 dz \left[g^{(2)}\left(x, \frac{1-z}{z} x, k_\perp^2\right) \right. \\
&\quad \left. - \frac{1}{2} g^{(2)}(zx, (1-z)x, k_\perp^2) \right] \gamma_{g \rightarrow gg}(z) \theta(k_\perp^2 - Q_0^2)
\end{aligned}$$

³It is convenient to visualize the initial $q\bar{q}$ pair (25) as a single incoming 'gluon' with momentum P , i.e. with $x_0 = 1$ and invariant mass Q (c.f Fig. 3).

$$\begin{aligned}
& + \frac{\lambda_\chi(k_\perp^2)}{2\pi} \int_0^1 dz \left[\frac{1}{z} g\left(\frac{x}{z}, k_\perp^2\right) - g(x, k_\perp^2) \right] \gamma_{g \rightarrow g\chi}(z) \\
& - \frac{\lambda_\chi(k_\perp^2)}{2\pi} \left(\frac{\Lambda^2}{k_\perp^2} \right) 8\pi^2 c_{gg \rightarrow \chi} \int_0^1 dz g^{(2)}\left(x, \frac{1-z}{z}x, k_\perp^2\right) \gamma_{\chi \rightarrow gg}(z) .
\end{aligned} \tag{38}$$

This equation reflects the probabilistic parton cascade interpretation of the LLA [34, 35, 36], in which the change of the gluon distribution on the left hand side is governed by the balance of gain (+) and loss (−) terms on the right hand side. Notice that (38) is free of infrared divergences, because the singularities in (33) at $z = 0$ and $z = 1$ cancel between gain and loss terms. A diagrammatic illustration of these gain and loss terms is shown in Fig. 4. Also notice that the gluon fusion terms (second and fourth term) involve the 2-gluon distribution $g^{(2)}(x_1, x_2, k_\perp^2)$, the presence of which causes the evolution equation to be non-linear.

By means of a Mellin transformation the multiple convolutions of z -integrals inherent in the iteration of eq. (38) can be converted into products of independent successive interaction probabilities. Let me define the gluon distribution in the *moment representation* as

$$g(\omega, k_\perp^2) := \int_0^1 dx x^\omega g(x, k_\perp^2) = \int_0^\infty dy e^{-\omega y} [xg(x, k_\perp^2)] , \tag{39}$$

where $y = \ln(1/x)$, in which the variable ω is conjugate to $\ln(1/x)$, implying that the low x behaviour is determined by small values of ω . Analogously, the 2-gluon distribution is represented as

$$g^{(2)}(\omega, z, k_\perp^2) := \int_0^1 dx x^\omega g^{(2)}\left(x, \frac{1-z}{z}x, k_\perp^2\right) , \tag{40}$$

which carries an additional z -dependence. In general $g^{(2)}$ is a complicated correlation function not available in analytical form, except for certain special cases [27, 37]. It is therefore inevitable on an analytical level to assume a phenomenological form of $g^{(2)}$ that allows to convert eq. (38) into a tractable linear form. This can be achieved with the following ansatz of product form [28, 38]

$$g^{(2)}\left(x, \frac{1-z}{z}x, k_\perp^2\right) = \rho(k_\perp^2) g\left(x, k_\perp^2\right) g\left(\frac{1-z}{z}x, k_\perp^2\right) , \tag{41}$$

where $\rho(k_\perp^2)$ is a parameter that characterizes the magnitude of the probability for finding two gluons at the same point in phase-space, depending on their typical transverse size $r_\perp \sim 1/k_\perp$. Since the 2-gluon correlation must become substantial when the number of gluons per unit area $n_g/(\pi R_\perp^2)$ becomes so large that the gluons overlap spatially ($R_\perp \approx 0.5 - 1$ fm), one expects that $\rho = O(1)$ when $k_\perp^2 \approx Q_0^2$ ($Q_0 = 1$ GeV), and monotonically increasing as

$k_{\perp}^2 \rightarrow \Lambda^2$. Using (41) in (40), the 2-gluon distribution in the moment representation can be approximated in the soft limit ($z \ll 1$) as

$$g^{(2)}(\omega, z, k_{\perp}^2) \approx \rho(k_{\perp}^2) \frac{z^{\omega}}{\omega} g(\omega, k_{\perp}^2). \quad (42)$$

In the moment representation the evolution equation (38) now becomes an linear algebraic equation for the Mellin transformed gluon distribution:

$$k_{\perp}^2 \frac{\partial}{\partial k_{\perp}^2} g(\omega, k_{\perp}^2) = \gamma(\omega, k_{\perp}^2) g(\omega, k_{\perp}^2), \quad (43)$$

where $\gamma(\omega, k_{\perp}^2)$ plays the role of a generalized *anomalous dimension*,

$$\begin{aligned} \gamma(\omega, k_{\perp}^2) &= \frac{\alpha_s(k_{\perp}^2)}{2\pi} \theta(k_{\perp}^2 - Q_0^2) \left[A_{g \rightarrow gg}(\omega) - \left(\frac{\Lambda^2}{k_{\perp}^2} \right) A_{gg \rightarrow g}(\omega) \right] \\ &\quad + \frac{\lambda_{\chi}(k_{\perp}^2)}{2\pi} \left[A_{g \rightarrow g\chi}(\omega) - \left(\frac{\Lambda^2}{k_{\perp}^2} \right) A_{gg \rightarrow \chi}(\omega) \right] \\ &\equiv \gamma_{QCD}(\omega, k_{\perp}^2) + \gamma_{\chi}(\omega, k_{\perp}^2). \end{aligned} \quad (44)$$

The functions $A(\omega)$ are given by

$$\begin{aligned} A_{g \rightarrow gg}(\omega) &= 2 C_A \left[\frac{11}{12} + \frac{1}{\omega} - \frac{2}{\omega+1} + \frac{1}{\omega+2} - \frac{1}{\omega+3} - S(\omega) \right] \\ A_{gg \rightarrow g}(\omega) &= \frac{\pi^2 \rho}{\omega} A_{g \rightarrow gg}(\omega) \\ A_{g \rightarrow g\chi}(\omega) &= \frac{1}{4} \left[\frac{3}{2} - \frac{1}{\omega+1} - \frac{1}{\omega+2} - 2S(\omega) \right] \\ A_{gg \rightarrow \chi}(\omega) &= \frac{\pi^2 \rho}{2\omega} \left[\frac{1}{\omega+1} - \frac{2}{\omega+2} - \frac{2}{\omega+3} \right]. \end{aligned} \quad (45)$$

where $S(\omega) = \psi(\omega+1) - \psi(1)$ with the Digamma function $\psi(z) = d[\ln \Gamma(z)]/dz$ and $-\psi(1) = \gamma_E = 0.5772$ the Euler constant.

The anomalous dimension $\gamma(\omega, k_{\perp}^2)$, eq. (44), reduces at $k_{\perp}^2 \gg \Lambda^2$ to γ_{QCD} , the QCD anomalous dimension in the LLA [33], since in this kinematic region $\kappa(\chi) = 1$ and therefore $\lambda_{\chi} = 0$. However, at $k_{\perp}^2 \simeq Q_0^2$, $\lambda_{\chi}(k_{\perp}^2)$ becomes non-zero, so that the evolution of the gluon distribution receives modifications due to the coupling of gluons to the χ -field. In the region $Q_0^2 > k_{\perp}^2 \geq \Lambda^2$, the perturbative QCD contributions $\propto \alpha_s$ vanish per construction, so that the gluons solely interact with the χ -field, the coupling to which increases, because $\kappa \rightarrow 0$, i.e. $\lambda_{\chi} \rightarrow 1$. This behaviour is evident in Fig. 5, which shows $\gamma(\omega, k_{\perp}^2)$ versus ω for different values of k_{\perp}^2 .

The formal solution of eq. (43) is

$$g(\omega, k_{\perp}^2) = \exp \left\{ \int_{k_{\perp}^2}^{Q^2} \frac{dk'_{\perp}{}^2}{k'_{\perp}{}^2} \gamma(\omega, k'_{\perp}{}^2) \right\} \quad (46)$$

from which the x distribution can be reconstructed by considering the inverse Mellin transform

$$x g(x, k_{\perp}^2) = \frac{1}{2\pi i} \int_C d\omega x^{-\omega} g(\omega, k_{\perp}^2), \quad (47)$$

where ω is now a complex variable and the contour of the integration C runs parallel to the imaginary axis. For the full anomalous dimension (44) this inversion must be done numerically [39].

3.2 Analytical estimates for x -spectra and gluon multiplicity

To exhibit the main features of the evolution of the gluon distribution in the presence of the χ -field, it is instructive to make some analytic estimates. Of particular interest is the low x -region, because the soft, small x gluons are most preferably radiated, but at the same time take away only a very small portion of the total energy. For simplicity I will divide the kinematic range of the k_{\perp}^2 -evolution into two distinct domains as indicated in Fig. 2:

- (i) $Q^2 \geq k_{\perp}^2 > Q_0^2$ and $k_{\perp}^2/\Lambda^2 \gg 1$: In this region $\lambda_{\chi} \simeq 0$ and $\partial\lambda_{\chi}/\partial \ln k_{\perp}^2 \simeq 0$, so that (44) reduces to

$$\gamma(\omega, k_{\perp}^2) = \frac{\alpha_s(k_{\perp}^2)}{2\pi} A_{g \rightarrow gg}(\omega). \quad (48)$$

- (ii) $Q_0^2 \geq k_{\perp}^2 \geq \Lambda^2$ and $k_{\perp}^2/\Lambda^2 \rightarrow 1$: Here $\lambda_{\chi} \rightarrow (4\pi)^{-1}$ and $\partial\lambda_{\chi}/\partial \ln k_{\perp}^2 > 0$, in which case (44) becomes

$$\gamma(\omega, k_{\perp}^2) = \frac{\lambda_{\chi}(k_{\perp}^2)}{2\pi} \left[A_{g \rightarrow g\chi}(\omega) - \left(\frac{\Lambda^2}{k_{\perp}^2} \right) A_{gg \rightarrow \chi}(\omega) \right]. \quad (49)$$

As stated before, the low x region corresponds to the limit $\omega \rightarrow 0$, so that an expansion of $\gamma(\omega, k_{\perp}^2)$ around $\omega = 0$ gives the dominant contributions at small x . Up to to order ω one has in the region (i)

$$k_{\perp}^2 \frac{\partial}{\partial k_{\perp}^2} \ln g(\omega, k_{\perp}^2) = \frac{\alpha_s(k_{\perp}^2)}{2\pi} \left[2C_A \left(\frac{1}{\omega} - \frac{11}{12} \right) \right] \equiv \gamma^{(i)}(\omega, k_{\perp}^2), \quad (50)$$

whereas in the region (ii) one gets in the same order of approximation

$$k_{\perp}^2 \frac{\partial}{\partial k_{\perp}^2} \ln g(\omega, k_{\perp}^2) = -\frac{\lambda_{\chi}(k_{\perp}^2)}{2\pi} \rho \frac{\Lambda^2}{k_{\perp}^2} \left[\frac{8\pi^2}{3\omega} \right] \equiv \gamma^{(ii)}(\omega, k_{\perp}^2). \quad (51)$$

The accuracy of the expressions $\gamma^{(i)}$ and $\gamma^{(ii)}$ in the relevant range of ω is exhibited in Fig. 6, where the exact expression $\gamma(\omega, k_{\perp}^2)$ is compared to the small- ω expansions (50) and (51) at large and small k_{\perp}^2 . Evidently the approximation is rather good for $\omega < 2$.

Eqs. (46) and (47) can now be solved analytically with the saddle point method. The k_{\perp}^2 -dependence of α_s is given in (34) and for $\lambda_{\chi} = \tilde{\xi}_{\chi}^2/(4\pi)$, eq. (35), I will use here the form

$$\lambda_{\chi}(k_{\perp}^2) = \frac{\theta(Q_0^2 - k_{\perp}^2)}{4\pi} \frac{\ln(Q_0^2/k_{\perp}^2)}{\ln(Q_0^2/\Lambda^2)}, \quad (52)$$

which has the required properties that $\lambda_{\chi} = 0$ ($\tilde{\xi}_{\chi} = 0$) for $k_{\perp}^2 \geq Q_0^2$ and $\lambda_{\chi} \rightarrow (4\pi)^{-1}$ ($\tilde{\xi}_{\chi} \rightarrow 1$) for $k_{\perp}^2 \rightarrow \Lambda^2$ (as before $\tilde{\xi}_{\chi}$ denotes the Fourier transform of $\xi(\chi)$ in eq. (8)).

Introducing the variables \hat{t} for the region (i) and \hat{u} for the region (ii),

$$\begin{aligned} \hat{t}(k_{\perp}^2) &= \int_{k_{\perp}^2}^{Q^2} \frac{dk'_{\perp}{}^2}{k'_{\perp}{}^2} \frac{\alpha_s(k'_{\perp}{}^2)}{2\pi} = \frac{1}{2\pi b} \ln \left[\frac{\ln(Q^2/\Lambda^2)}{\ln(k_{\perp}^2/\Lambda^2)} \right] \\ \hat{u}(k_{\perp}^2) &= \int_{k_{\perp}^2}^{Q_0^2} \frac{dk'_{\perp}{}^2}{k'_{\perp}{}^2} \left(\frac{\lambda_{\chi}(k'_{\perp}{}^2)}{2\pi} \rho \frac{\Lambda^2}{k'_{\perp}{}^2} \right) = \frac{\rho}{8\pi^2} \frac{1 - (Q_0^2/k_{\perp}^2) (1 - \ln(Q_0^2/k_{\perp}^2))}{(Q_0^2/\Lambda^2) \ln(Q_0^2/\Lambda^2)}, \end{aligned} \quad (53)$$

the combination of (46) and (47) yields for the kinematic domains (i), respectively (ii):

$$\begin{aligned} xg(x, \hat{t}) &= \frac{1}{2\pi i} \int_C d\omega \exp \left[\omega y + \nu^{(i)}(\omega) \hat{t} \right] g(\omega, 0), \quad \nu^{(i)}(\omega) = 2C_A \left(\frac{1}{\omega} - \frac{11}{12} \right) \\ xg(x, \hat{u}) &= \frac{1}{2\pi i} \int_C d\omega \exp \left[\omega y + \nu^{(ii)}(\omega) \hat{u} \right] g(\omega, 0), \quad \nu^{(ii)}(\omega) = \frac{8\pi^2}{3\omega}, \end{aligned} \quad (54)$$

where $y = \ln(1/x)$. The saddlepoint $\omega_S^{(i)}$ of the integrand in (54) is determined by the condition

$$\frac{d}{d\omega} \left\{ \omega y + \nu^{(i)} \hat{t} \right\} \Big|_{\omega=\omega_S^{(i)}} = 0 \quad (55)$$

and similarly $\omega_S^{(ii)}$. Using the method of steepest descent then gives the following results.

(i) In the region $Q^2 \geq k_{\perp}^2 \geq Q_0^2$:

$$xg(x, k_{\perp}^2) \Big|_{Q^2 \geq k_{\perp}^2 \geq Q_0^2} = N_1(x) + G_1(x, k_{\perp}^2) \exp \left[-\frac{11C_A}{12\pi b} H_1(k_{\perp}^2) \right] \exp \left[\sqrt{\frac{4C_A}{\pi b} H_1(k_{\perp}^2) \ln \left(\frac{1}{x} \right)} \right]$$

$$N_1(x) = xg(x, k_{\perp}^2 = Q^2) = \delta(1-x) \delta(k_{\perp}^2 - Q^2)$$

$$\begin{aligned}
G_1(x, k_\perp^2) &= \frac{1}{\sqrt{4\pi}} \left[\frac{C_A}{\pi b} H_1(k_\perp^2) \right]^{1/4} \left[\ln \left(\frac{1}{x} \right) \right]^{-3/4} \\
H_1(k_\perp^2) &= \ln \left[\frac{\ln(Q^2/\Lambda^2)}{\ln(k_\perp^2/\Lambda^2)} \right].
\end{aligned} \tag{56}$$

(ii) In the region $Q_0^2 \geq k_\perp^2 \geq Q_0^2$:

$$\begin{aligned}
x g(x, k_\perp^2) \Big|_{Q_0^2 \geq k_\perp^2 \geq \Lambda^2} &= N_2(x) - G_2(x, k_\perp^2) \exp \left[\sqrt{\frac{4\rho}{3}} H_2(k_\perp^2) \ln \left(\frac{1}{x} \right) \right] \\
N_2(x) &= x g(x, k_\perp^2 = Q_0^2) \\
G_2(x, k_\perp^2) &= \frac{1}{\sqrt{4\pi}} \left[\frac{\rho}{3} H_2(k_\perp^2) \right]^{1/4} \left[\ln \left(\frac{1}{x} \right) \right]^{-3/4} \\
H_2(k_\perp^2) &= \frac{1 - (Q_0^2/k_\perp^2) (1 - \ln(Q_0^2/k_\perp^2))}{(Q_0^2/\Lambda^2) \ln(Q_0^2/\Lambda^2)}.
\end{aligned} \tag{57}$$

In Fig. 7 the x -spectra of (56) and (57) are shown for different values of k_\perp^2 with fixed $Q_0 = 1$ GeV. Two different initial distributions were chosen to start the evolution from $k_\perp^2 = (3.5 \text{ GeV})^2$, one flat in rapidity and the other one a Gaussian form. The parameter ρ introduced in (41) was set equal to one. For $k_\perp^2 \gtrsim Q_0^2$ the gluon distribution $xg(x, k_\perp^2)$ is just the well known LLA solution with its strong increase at small x as k_\perp^2 decreases. For $k_\perp^2 < Q_0^2$ however, the effect is reversed such that $g(x, k_\perp^2)$ decreases as k_\perp^2 falls below Q_0^2 . This suppression, which is particularly substantial at small x , reflects the "condensation" of gluons in the collective background field χ .

The k_\perp^2 -dependence of the total gluon multiplicity can also be estimated in the above approximation. The gluon multiplicity is given by the $\omega = 0$ moment,

$$N_g(k_\perp^2) = g(\omega = 0, k_\perp^2) = \int_0^1 dx g(x, k_\perp^2). \tag{58}$$

Using eqs. (43)-(45), one arrives in the soft limit ($z \ll 1$) [40, 37] at the following integral equations that govern the approximate behaviour of the gluon multiplicity for the two cases (i) and (ii):

$$\begin{aligned}
(i) \quad k_\perp^2 \frac{\partial}{\partial k_\perp^2} N_g(k_\perp^2) &= \frac{\alpha_s(k_\perp^2)}{2\pi} \left\{ 2C_A \int_{k_\perp^2}^{Q^2} \frac{dk'^2}{k'^2} N_g(k'^2) - \frac{1}{2} N_g(k_\perp^2) \right\} \\
(ii) \quad k_\perp^2 \frac{\partial}{\partial k_\perp^2} N_g(k_\perp^2) &= -\frac{\lambda_\chi(k_\perp^2)}{2\pi} \left(8\pi^2 c_{gg \rightarrow \chi} \frac{\Lambda^2}{k_\perp^2} \right) \int_{k_\perp^2}^{Q_0^2} \frac{dk'^2}{k'^2} N_g(k'^2).
\end{aligned} \tag{59}$$

On account of the k_{\perp}^2 -dependence of α_s (34) and λ_{χ} (52), the corresponding solutions are obtained as:

$$(i) \quad N_g(k_{\perp}^2) \Big|_{Q^2 \geq k_{\perp}^2 \geq Q_0^2} = N_g(Q^2) \left(\frac{\ln(Q^2/\Lambda^2)}{\ln(k_{\perp}^2/\Lambda^2)} \right)^{-1/4} \frac{\exp \left[2 \sqrt{(C_A/\pi b) \ln(Q^2/\Lambda^2)} \right]}{\exp \left[2 \sqrt{(C_A/\pi b) \ln(k_{\perp}^2/\Lambda^2)} \right]}$$

$$(ii) \quad N_g(k_{\perp}^2) \Big|_{Q_0^2 \geq k_{\perp}^2 \geq \Lambda^2} = N_g(Q_0^2) \exp \left[-\frac{\rho}{2} \frac{\Lambda^2}{k_{\perp}^2} \frac{1 + [1 + \ln(k_{\perp}^2/Q_0^2)]^2 - 2k_{\perp}^2/Q_0^2}{\ln(Q_0^2/\Lambda^2)} \right] \quad (60)$$

In the region (i) $Q^2 \geq k_{\perp}^2 > Q_0^2$, the multiplicity coincides with the QCD result [33], characterized by a rapid growth as the gap between the hard scale Q^2 and k_{\perp}^2 increases. On the other hand, in the region (ii) $Q_0^2 \geq k_{\perp}^2 > \Lambda^2$, the multiplicity becomes strongly damped. The exponent is always negative so that the number of gluons rapidly decreases and vanishes at $k_{\perp}^2 = 0$, ensuring that no gluons and therefore no color fluctuations exist at distances $R \gtrsim \Lambda^{-1}$. This behaviour is evident in Fig. 8, where $N_g(k_{\perp}^2)$ is plotted versus Λ^2/k_{\perp}^2 , starting from $\Lambda^2/Q^2 \ll 1$.

It must be emphasized that the *perturbative* evolution of gluons is cut off at Q_0^2 , and in the transition region $Q_0^2 \geq k_{\perp}^2 > \Lambda^2$ the evolution is purely *non-perturbative*, although it is described here as an extension of the perturbative evolution above Q_0^2 and treated on the same footing.

3.3 Flux tube configurations of gluons interacting with the mean field χ

In Secs. 3.1 and 3.2 the evolution of the gluon configuration between the fragmenting $q\bar{q}$ pair was analyzed in terms of the non-perturbative modification as a function of $\lambda_{\chi}(k_{\perp}^2) = \tilde{\xi}_{\chi}^2/(4\pi)$. However, the coupling strength λ_{χ} or $\tilde{\xi}_{\chi}$ between the gluon field and the χ -field must be determined by the dynamics itself, since $\tilde{\xi}_{\chi}$ is the Fourier transform of the χ -dependent coupling function $\xi(\chi)$ in eq. (8).

The dynamics is governed by the the coupled system of equations eqs. (19)-(21), which can now be solved numerically by utilizing the definition (36) together with the general solution for the gluon distribution given by (46) and (47). To do so, one obtains the expectation value of eq. (20) by multiplying with the multigluon state vector $\langle P|$ and $|P\rangle$ from the left and right, respectively. In the mean field approximation, $\chi = \bar{\chi}$ is a c -number function, so that this operation affects only the $F_{\mu\nu}F^{\mu\nu}$ term which gives the gluon distribution by virtue of (36). With the explicit solution of the gluon distribution (56) and

(57) inserted, the remaining task is to solve the single equation (20) for the χ -field. (Recall that the equation (21) for the U -field couples only to χ and is in principle readily solved once the solution for χ is known.)

An interesting phenomenological application [20, 22, 41] is to calculate the *string tension* t , which characterizes the linearly rising potential between the $q\bar{q}$ -pair due to the gluon interactions. usually obtained by fitting heavy quarkonium spectra [42] with a non-relativistic potential of the form

$$V_{q\bar{q}}(r) = -\frac{a}{r} + t r^2, \quad (61)$$

where $a = 4\alpha_s/3$. Typical fit values for the string constant t range from 750 MeV/fm to 950 MeV/fm.

Here I shall estimate the string constant within the present approach on the basis of the equations of motion (19)-(21). Similar calculations have been done earlier in the framework of the static MIT bag model [43] and the Friedberg-Lee soliton model [22, 41].

In the following I will consider the fragmentation of a heavy $q\bar{q}$ pair within an *adiabatic* approximation. That is, a quasistatic treatment is employed which neglects the motion of the $q\bar{q}$ pair and considers the instantaneous gluon configuration in between the pair. This should provide is a reasonable approximation, because one can view the i^{th} gluon as being emitted from the $q\bar{q}$ pair plus gluons g_1, g_2, \dots, g_{i-1} , with the spatial coordinates of these "sources" being frozen during the emission of the gluon i [44]. In a space-time picture of the fragmentation of the $q\bar{q}$ and its emitted gluons it is the change of the typical transverse momenta k_\perp or transverse separation $r_\perp \propto k_\perp^{-1}$ of gluons which governs the dynamical transition from short distance, unconfined regime to long distance, confined stage [2], because there must be a critical separation of color charges beyond which the total color is screened. In the present case, the role of this non-perturbative phenomenon is played by the χ -field. In the adiabatic approximation, there is no explicit dependence on the longitudinal variables here, because the separation in the transverse plane is independent of when during the cascade, or where along the jet axis, a gluon was produced [45].

Thus, within the adiabatic treatment, one may use the separation $R_{q\bar{q}}$ of the receding $q\bar{q}$ as a measure for the typical gluon transverse momenta $k_\perp^2 \approx R_{q\bar{q}}^{-2}$. By minimizing the energy per unit length of this system, one obtains then for each gluon configuration at a given $R_{q\bar{q}}$ the form of χ and the string tension t . The total energy per unit length, the

string tension t , receives contributions from both the χ -field in the low energy regime and the gluon field in the high energy domain, which on account of the trace anomaly (3) is given by:

$$t \equiv \frac{E}{R_{q\bar{q}}} = \int dA \left[\frac{1}{2} |\nabla\chi|^2 + V(\chi) \right] + \int dA \kappa(\chi) \langle P | \frac{\beta(\alpha_s)}{4\alpha_s} F_{\mu\nu,a} F_a^{\mu\nu} | P \rangle. \quad (62)$$

Here A is the cross-sectional area of the flux tube of the gluons between the $q\bar{q}$, perpendicular to $R_{q\bar{q}}$. In one loop order the beta-function is $\beta = -b\alpha_s^2$ with $b = 33/(12\pi)$ for $N_f = 0$. Then, by using eq. (36) to express the second integral in terms of the gluon distribution $g(x, k_\perp^2)$, assuming cylindrical symmetry along the $R_{q\bar{q}}$ axis, and minimizing t with respect to χ , one arrives at the following non-linear integro-differential equation (r is the radial coordinate perpendicular to $R_{q\bar{q}}$):

$$- \left[\frac{d^2}{dr^2} + \frac{1}{r} \frac{d}{dr} \right] \chi(r) + \frac{\partial V(\chi)}{\partial \chi} + (P^+)^2 \frac{b}{2} I_g(R_{q\bar{q}}) \int dr r \kappa(\chi) = 0, \quad (63)$$

where

$$I_g(R_{q\bar{q}}) = \int_{1/R_{q\bar{q}}}^{(P^+)^2} d^2 k_\perp \alpha_s(k_\perp^2) \int_0^1 dx x g(x, k_\perp^2). \quad (64)$$

In pulling I_g out of the r -integral, it is assumed that the spatial distribution of gluons is approximately homogenous. Eq. (63) determines the energetically most favorable flux tube configuration. However, a physical meaningful flux tube solution has to satisfy the *constraint* that the system as a whole, $q\bar{q}$ plus gluons, must form a global color singlet, implying that all of the color flux that originates from the q must be directed towards the \bar{q} . In other words, the total color electric flux through a plane between the q and \bar{q} must be equal the color charge $Q_q = g_s T_a$ on one of them [22, 41]. This translates into the requirement that the gluons in the flux tube stretched between q and \bar{q} with certain $R_{q\bar{q}}$ carries a total color charge squared that is equal to Q_q^2 , the one of $q\bar{q}$. Define

$$\phi_g = \frac{(P^+)^2}{A} \int d^2 r J_g(R_{q\bar{q}}), \quad (65)$$

where A is the cross-sectional area of the flux tube, and

$$J_g(R_{q\bar{q}}) = \int_{1/R_{q\bar{q}}}^{(P^+)^2} d^2 k_\perp \int_0^1 dx g(x, k_\perp^2), \quad (66)$$

is the total number of gluons radiated from the initial point of $q\bar{q}$ -production up to $R_{q\bar{q}}$. Then the above constraint then reads

$$\phi_g \stackrel{!}{=} Q_q^2 = \langle g_s^2 T_a \cdot T_a \rangle = \frac{16\pi}{3} \alpha_s(k^2) \Big|_{k^2=R_{q\bar{q}}^{-2}}. \quad (67)$$

Combining eqs. (63)-(67), one arrives at

$$- \left[\frac{d^2}{dr^2} + \frac{1}{r} \frac{d}{dr} \right] \chi(r) + \frac{\partial V(\chi)}{\partial \chi} + \frac{8\pi}{3} b \alpha_s(R_{q\bar{q}}^{-2}) \frac{I_g(R_{q\bar{q}})}{J_g(R_{q\bar{q}})} \int dr r \kappa(\chi) = 0, \quad (68)$$

which is now independent of the overall boost momentum (P^+), and thus of the initial hard scale $Q^2 = (P^+)^2$, as it should be.

Solving eq. (68) numerically [46], subject to the the boundary conditions $\chi'(0) = 0$ and $\chi(\infty) = \chi_0$ yields the solutions for t , χ and $\kappa(\chi)$ shown in Fig. 9. The reasonable parameter values [17] $\chi_0 = f_\pi$ and bag constant $B = (150 \text{ MeV})^4$ were chosen for $V(\chi)$, eq. (14), and the coupling function κ was taken of the form (11). One sees that with increasing separation $R_{q\bar{q}}$ of q and \bar{q} , the gluons first multiply which results in a growing string tension, but then gluon condensation sets in, yielding a saturating behaviour of t with the string constant approaching $t \simeq 1 \text{ GeV/fm}$ (Fig. 9a). For $R_{q\bar{q}} \approx 1 \text{ fm}$ the gluon field is completely confined within a flux tube of radius $r \simeq 1 \text{ fm}$ (Fig. 9b). For comparison, a simple estimate within the MIT bag model [43] gives $t = 910 \text{ MeV/fm}$, but a rather large tube radius of 1.6 fm. Detailed calculations with in the soliton model [22] gave qualitatively similar results. Finally, Fig. 10 shows in correspondance to Fig 9b the form of the potential $V(\chi) \equiv V(\chi, U)|_{m_q=0}$, defined in eq. (14), and the effective squared mass $M^2(\chi) = d^2V(\chi)/d\chi^2$ for the same parameter values as above.

4. SUMMARY AND OUTLOOK

The effective QCD field theory approach presented here to describe the dynamics of high energy partons in the presence of a collective confinement field provides a framework that has the potential to be developed towards a systematic description of the hadronization mechanism. The corresponding effective action has been constructed such that it

- (i) incorporates both parton and hadron degrees of freedom;
- (ii) recovers the exact QCD (Yang-Mills) action with its symmetry properties at short space-time distances;
- (iii) merges into an effective low energy description of hadronic degrees of freedom at large distances;

- (iv) allows for a dynamical description of parton-hadron conversion on the basis of the resulting equations of motion.

As an exemplary demonstration, the approach was applied to the evolution of a fragmenting $q\bar{q}$ pair with its generated gluon distribution, starting from a large hard scale Q^2 all the way downwards to Λ^2 . The transformation of the initially high virtual gluons to a gluon condensate field χ was studied in terms of the coupled evolution of the gluon distribution and the mean field χ . The solution of the equations of motion yields color flux tube configurations with an associated energy per unit area (string tension) of about 1 GeV/fm, consistent with the common estimates.

In perspective, important points to be addressed in the future, are:

- (i) The establishment of the relation with the exact renormalization group equation for the effective action as derived by Reuter and Wetterich [5] is desirable. This would allow to quantify the effect of consecutively integrating out all quantum fluctuations of gluons and quarks with momenta larger than some infra-red cut-off scale Q_0 , the variation of which determines the confinement dynamics.
- (ii) With the inclusion of quark degrees of freedom and possibly quantum fluctuations of the χ - and U -fields, one could calculate e.g. the mass spectrum of glueball and meson excitations as physical hadrons. This would provide a complete description from a physical initial state, via a not directly observable deconfined partonic stage, up to the formation of observable hadronic excitations.
- (iii) Ultimately one would like to address the microscopic dynamics in full 6-dimensional phase-space [47], with explicit inclusion of the color degrees of freedom and the local color structure. This could be realized in a transport theoretical formulation similar as in Ref. [48], in which the partons propagate with a modified propagator that embodies the effects of the mean field χ in the effective mass. As the confining field becomes significant the effective mass increases and asymptotically becomes infinite so that the propagation of color fluctuations ceases.
- (iv) The possible applications are manifold. One particular interest is the expected (non)equilibrium QCD phase transition in high energy systems as in heavy ion collisions or the early universe, an issue which could be addressed along the lines of

Campbell, Ellis and Olive [17] in combination with the space-time evolution of the multi-parton system [47] in the presence of the collective field.

Acknowledgements

I thank J. Ellis, H.-T. Elze and G. Veneziano for valuable suggestions. Thanks also to L. Wilets and W. Hofer for providing the computer code for the flux tube calculation.

APPENDIX A

For completeness a "derivation" of the evolution equation (26) is given in the spirit of Lipatov [49]. The full propagator of a single gluon of momentum k may be represented as

$$D_{\mu\nu}(k) = \frac{d_{\mu\nu}(k)}{k^2 (1 + \Pi(k^2))} \equiv \frac{D_{\mu\nu}^0(k)}{1 + \Pi(k^2)}, \quad (69)$$

where $D_{\mu\nu}^0 = d_{\mu\nu}/k^2$ is the free propagator, and with the choice of gauge for the gluon fields $\eta \cdot A = 0$,

$$d_{\mu\nu}(k) = g_{\mu\nu} - \frac{k_\mu \eta_\nu + k_\nu \eta_\mu}{k \cdot \eta}, \quad d_{\mu\mu}(k) = 2 \quad (70)$$

and $k^\mu d_{\mu\nu}(k)|_{k^2=0} = 0$ guarantees that only 2 physical (transverse) gluon polarizations propagate on mass shell. The self-energy part

$$\Pi(k^2) = \Pi_{g \leftrightarrow g}(k^2) + \Pi_{g \leftrightarrow \chi}(k^2) \quad (71)$$

contains both the gluon self-interactions and the "medium" corrections due to the coupling to the confining background field χ . Expanding $\Pi_{g \leftrightarrow g}$ and $\Pi_{g \leftrightarrow \chi}$ in powers of the squared couplings g_s^2 and ξ_χ^2 , respectively, the contribution to one loop order is determined by the total gluon "decay" probability, i.e. the probability of losing a gluon out of a momentum space element between k^2 and $k^2 + dk^2$:

$$w_g(k^2) = \frac{\partial}{\partial \ln(k'^2/\Lambda^2)} \left[\Pi_{g \leftrightarrow g}(k'^2) + \Pi_{g \leftrightarrow \chi}(k'^2) \right]_{k'^2=k^2} \equiv w_{g \leftrightarrow g} + w_{g \leftrightarrow \chi}. \quad (72)$$

Here, $w_{g \leftrightarrow g}$ and $w_{g \leftrightarrow \chi}$ are the inclusive probabilities for a gluon to emit (absorb) another gluon, due to the self-interaction, respectively the interaction with the χ -field, corresponding to the diagrams in Fig. 4,

$$\begin{aligned} w_{g \leftrightarrow g}(k^2) &= \int_0^1 dx \int_x^1 \frac{dx'}{x'} \left[w_{g \rightarrow gg}(x', x, k^2) + w_{gg \rightarrow g}(x', x, k^2) \right] \\ w_{g \leftrightarrow \chi}(k^2) &= \int_0^1 dx \int_x^1 \frac{dx'}{x'} \left[w_{g \rightarrow g\chi}(x', x, k^2) + w_{gg \rightarrow \chi}(x', x, k^2) \right]. \end{aligned} \quad (73)$$

The individual contributions in square brackets $w(x_1, x_2, k^2)$ can be obtained in the standard fashion [50, 51] by evaluating the cross-section ratios (c.f. Appendix B)

$$\frac{k_\perp^2}{\sigma^{(0)}} \frac{d\sigma^{(1)}}{dz dk_\perp^2} = \frac{g^2}{8\pi^2} \gamma_{a \rightarrow bc}(z), \quad (74)$$

where g denotes the appropriate coupling for the process under consideration (here $g = g_s$ or $g = \xi_\chi$), $\sigma^{(0)}$ is the Born cross-section for the production of a gluon a and $\sigma^{(1)}$ represents the first order correction associated with the "decay" $a \rightarrow bc$.

For the process $g \rightarrow gg$ and its reversal $gg \rightarrow g$ the probability distributions (33) are well known [50, 38]. Assigning the momentum fractions as $x_1 \rightarrow x_2, (x_1 - x_2)$ for $g \rightarrow gg$ and $x_1, (x_2 - x_1) \rightarrow x_2$ for $gg \rightarrow g$, one has

$$\begin{aligned} w_{g \rightarrow gg}(x_1, x_2, k^2) &= \frac{\alpha_s(k^2)}{2\pi} \gamma_{g \rightarrow gg} \left(\frac{x_2}{x_1} \right) \\ w_{gg \rightarrow g}(x_1, x_2, k^2) &= \frac{\alpha_s(k^2)}{2\pi} \left[8\pi^2 c_{gg \rightarrow g} \frac{\Lambda^2}{k^2} \frac{x_1(x_2 - x_1)}{x_2^2} \right] \gamma_{g \rightarrow gg} \left(\frac{x_1}{x_2} \right), \end{aligned} \quad (75)$$

where in the second expression the factors in square brackets arise from the difference of phase-space and flux factors for fusions compared to branchings. The color factor is $c_{gg \rightarrow g} = 1/8$ and

$$\gamma_{g \rightarrow gg}(z) = 2C_A \left(z(1-z) + \frac{z}{1-z} + \frac{1-z}{z} \right), \quad (76)$$

where $C_A = N_c = 3$, and z is the fraction of x -values of daughter to mother gluons.

The new, additional processes are the friction process $g \rightarrow g\chi$, corresponding to energy-momentum transfer from gluons to the χ -field, and the fusion process $gg \rightarrow \chi$, by which two gluons couple color neutral to the χ -field and "annihilate" ⁴. As outlined in Appendix B, one arrives at (with the assignment $x_1 \rightarrow x_2, (x_1 - x_2)$ for $g \rightarrow g\chi$ and $x_1, (x_2 - x_1) \rightarrow x_2$ for $gg \rightarrow \chi$)

$$\begin{aligned} w_{g \rightarrow g\chi}(x_1, x_2, k^2) &= \frac{\lambda_\chi(k^2)}{2\pi} \gamma_{g \rightarrow g\chi} \left(\frac{x_2}{x_1} \right) \\ w_{gg \rightarrow \chi}(x_1, x_2, k^2) &= \frac{\lambda_\chi(k^2)}{2\pi} \left[8\pi^2 c_{gg \rightarrow \chi} \frac{\Lambda^2}{k^2} \frac{x_1(x_2 - x_1)}{x_2^2} \right] \gamma_{\chi \rightarrow gg} \left(\frac{x_1}{x_2} \right), \end{aligned} \quad (77)$$

where $c_{gg \rightarrow \chi} = 1/8$, and

$$\begin{aligned} \gamma_{g \rightarrow g\chi}(z) &= \frac{1}{4} \left(\frac{1+z^2}{1-z} \right) \\ \gamma_{\chi \rightarrow gg}(z) &= 8 \left(z^2 - z + \frac{1}{2} \right). \end{aligned} \quad (78)$$

⁴Since the conversion of partons into hadrons in the process of fragmentation is an irreversible process, the spontaneous production of gluons by the χ -field $\chi \rightarrow gg$, as well as the energy transfer from the χ -field to the gluons, $g\chi \rightarrow g$, are omitted. These latter interactions would counteract the transition, which certainly is possible in the sense of local fluctuations, but globally, and in the average, the parton-hadron conversion is a one-way process in the present context.

The total interaction probability w_g (72) determines via the unitarity condition (30) the Sudakov formfactor F_g ,

$$F_g(Q^2, k^2) = \exp \left[- \int_{k^2}^{Q^2} \frac{dk'^2}{k'^2} w_g(k'^2) \right] \quad (79)$$

which is the probability that a gluon does not at all interact (i.e. emit or absorb other gluons) while degrading its virtuality from Q^2 to k^2 .

The self-energy part (71) is now readily evaluated on the basis of eq. (72), and inserted in the representation (69), one obtains the single gluon propagator at one loop order,

$$D_{\mu\nu}(k) = D_{\mu\nu}^0(k) \left[1 + \int_{k^2}^{Q^2} \frac{dk'^2}{k'^2} \int_x^1 \frac{dx'}{x'} w(x', x, k^2) \right]. \quad (80)$$

The corresponding "jet calculus" [27] Greens function $D_g(x, k^2; x_0, Q^2)$ of eq. (26) describes how a system of gluons evolves in the variable x and the virtuality k^2 through the gluon self-interactions and in the presence of the confining background field χ . It is given by the convolution of the single gluon propagator (69) with the gluon distribution function $g(x, k^2)$. Defining

$$D_g(x, k^2; x_0, Q^2) \equiv g_{\mu\nu} D^{\mu\nu}(k) \otimes g(x, k^2), \quad (81)$$

the self-consistent iteration of one loop contributions to all orders within the LLA gives the evolution equation for the gluon distribution with respect to the variables x and k^2 :

$$\begin{aligned} k^2 \frac{\partial}{\partial k^2} g(x, k^2) &\equiv k^2 \frac{\partial}{\partial k^2} D_g(x, k^2; x_0, Q^2) \\ &= + \frac{\alpha_s(k^2)}{2\pi} \left\{ \int_x^1 \frac{dx'}{x'} g(x', k^2) \gamma_{g \rightarrow gg} \left(\frac{x}{x'} \right) - \frac{1}{2} g(x, k^2) \int_0^1 dz \gamma_{g \rightarrow gg}(z) \right\}_{k^2 \geq Q_0^2} \\ &\quad - \frac{\alpha_s(k^2)}{2\pi} \left(8\pi^2 \frac{\Lambda^2}{k^2} \right) \left\{ \int_0^1 dx' g^{(2)}(x, x', k^2) \Gamma_{gg \rightarrow g}(x, x', x + x') \right. \\ &\quad \left. - \frac{1}{2} \int_x^1 dx' g^{(2)}(x - x', x', k^2) \Gamma_{gg \rightarrow g}(x - x', x', x) \right\}_{k^2 \geq Q_0^2} \\ &\quad + \frac{\lambda_\chi(k^2)}{2\pi} \left\{ \int_x^1 \frac{dx'}{x'} g(x', k^2) \gamma_{g \rightarrow g\chi} \left(\frac{x}{x'} \right) - g(x, k^2) \int_0^1 dz \gamma_{g \rightarrow g\chi}(z) \right\} \\ &\quad - \frac{\lambda_\chi(k^2)}{2\pi} \left(8\pi^2 \frac{\Lambda^2}{k^2} \right) \left\{ \int_0^1 dx' g^{(2)}(x, x', k^2) \Gamma_{gg \rightarrow \chi}(x, x', x + x') \right\} \quad (82) \end{aligned}$$

where the factor 1/2 in the first (third) term arises from the indistinguishability of the two gluons emerging from (coming in) the branching (fusion) vertex. The function $g^{(2)}(x_1, x_2, k^2)$ denotes the 2-gluon density, and the gluon fusion functions Γ are defined in accord with

(75) and (77) as

$$\Gamma_{12 \rightarrow 3}(x_1, x_2, x_3) = c_{12 \rightarrow 3} \frac{x_1 x_2}{x_3^2} \gamma_{3 \rightarrow 12} \left(\frac{x_1}{x_3} \right) = c_{12 \rightarrow 3} \frac{x_1 x_2}{x_3^2} \gamma_{3 \rightarrow 21} \left(\frac{x_2}{x_3} \right). \quad (83)$$

with $x_3 = x_1 + x_2$. Changing to variables $(x, x_1, k^2) \rightarrow (x, z, k_\perp^2)$ and using (83), one immediately arrives at eq. (31).

APPENDIX B

Here I will outline the explicit calculation of the interaction probability densities $\gamma_{g \rightarrow g\chi}$ and $\Gamma_{gg \rightarrow \chi}$ that appear in the evolution equation (82) or (38) in addition to the usual probability densities $\gamma_{g \rightarrow gg}$ and $\Gamma_{gg \rightarrow g}$. Notice that the vertex corresponding to three gluons coupling to the χ -field is unphysical and therefore to be excluded, because χ is required to be a color singlet field. On the other hand, the coupling of four gluons to χ is possible, however in the LLA such diagrams are kinematically suppressed and can be neglected [2].

Let $\sigma^{(N)}$ denote the spin and color averaged cross-section for the production of a gluon at order N in perturbation theory. The probability distribution $\gamma_{a \rightarrow bc}$ in the variable $z = x_b/x_a$ for the emission of a gluon b in the process $a \rightarrow bc$, is the given by the ratio of cross-sections

$$\frac{1}{\sigma^{(0)}} \frac{d\sigma^{(1)}}{dz} = \frac{g^2}{8\pi^2} \gamma_{a \rightarrow bc}(z) \frac{dk_\perp^2}{k_\perp^2}, \quad (84)$$

where g is the appropriate coupling of the process, $\sigma^{(0)}$ is the lowest order cross-section for the production of a gluon a and $\sigma^{(1)}$ represents the first order correction associated with the "decay" $a \rightarrow bc$. The vertex function associated with the general $gg\chi$ coupling is easily obtained from the interaction Lagrangian $\mathcal{L}[\psi, \mathcal{A}, \chi]$, eq. (8), as:

$$V_{\mu\nu}^{ab}(k_1, k_2, k) = -\tilde{\xi}_\chi(k) \delta^{ab} \left[(k_1 \cdot k_2) g_{\mu\nu} - (1-a) k_{1\mu} k_{2\nu} \right] \quad (85)$$

where $\tilde{\xi}_\chi(k^2)$ denotes the Fourier transform of $\xi(\chi)$ in coordinate space, k_1, k_2 are the gluon momenta and the convention is that all four-momenta are directed into the vertex. The process $g \rightarrow g\chi$ gives then (setting $a = 1$):

$$\sigma^{(1)}(k_1^2) = \int \frac{d^3k}{(2\pi)^3 2k_0} \frac{2}{(k_1 \cdot k)^2} \sigma^{(0)}(k_1^2) |\overline{\mathcal{M}}|^2, \quad (86)$$

where

$$|\overline{\mathcal{M}}|^2 = \frac{1}{16} \sum_{a,a',b,b'} \sum_{s_1,s_2} V_{\mu\nu}^{ab} V_{\mu'\nu'}^{*a'b'} e^{*\mu}(s_1) e^{*\nu}(s_2) e^{\mu'}(s_1) e^{\nu'}(s_2), \quad (87)$$

where the factor $1/16$ in front results from the averaging over initial 2 transverse polarizations and 8 color degrees, and it is summed over final color and spin polarizations s_i . The sum over gluon polarizations s_1, s_2 must be performed over transverse polarizations only. This is achieved by the projection

$$\sum_{s_i} e^\mu(s_i) e^{*\nu}(s_i) = -g^{\mu\nu} + \frac{k^\mu k_i^\nu + k^\nu k_i^\mu}{(k \cdot k_i)} - \frac{k^2 k_i^\mu k_i^\nu}{(k \cdot k_i)^2}. \quad (88)$$

Assigning the momenta $k^\mu = (k^+, k^-, \vec{k}_\perp)$ of incoming (outgoing) gluon k_1 (k_2) and the momentum k transferred to the χ -field as

$$\begin{aligned} k_1 &= \left(k_1^+, 0, \vec{0}_\perp \right) \\ k_2 &= \left((1-z)k_1^+, \frac{k_\perp^2}{(1-z)k_1^+}, -\vec{k}_\perp \right) \\ k &= \left(zk_1^+, \frac{k_\perp^2}{zk_1^+}, \vec{k}_\perp \right), \end{aligned} \quad (89)$$

and carrying out the appropriate change of integration variables, the result is

$$\sigma^{(1)}(k_1^2) = \sigma^{(0)}(k_1^2) \frac{\tilde{\xi}_\chi^2}{8\pi^2} \int_{k_0^2}^{k_1^2} \frac{dk_\perp^2}{k_\perp^2} \int dz \left[\frac{1}{4} \left(1 - z + 2 \frac{z}{1-z} \right) \right]. \quad (90)$$

Hence, one can read off

$$\gamma_{g \rightarrow g\chi}(z) = \frac{k_\perp^2}{\sigma^{(0)}} \frac{d\sigma^{(1)}}{dz dk_\perp^2} = \frac{1}{4} \left(\frac{1+z^2}{1-z} \right). \quad (91)$$

In complete analogous manner the process $gg \rightarrow \chi$ can be calculated. The procedure is to evaluate $\chi \rightarrow gg$, with incoming momentum k and the outgoing momenta k_1 and k_2 . Using the formula (83) one obtains the 2-gluon fusion function for the reverse process $gg \rightarrow \chi$. The result is:

$$\Gamma_{gg \rightarrow \chi}(x_1, x_2, x_3) = c_{gg \rightarrow \chi} \frac{x_1 x_2}{x_3^2} \gamma_{\chi \rightarrow gg} \left(\frac{x_1}{x_3} \right), \quad (x_3 = x_1 + x_2), \quad (92)$$

$$\gamma_{\chi \rightarrow gg}(z) = 8 \left(z^2 - z + \frac{1}{2} \right). \quad (93)$$

References

- [1] A. H. Mueller (ed.), *Perturbative Quantum Chromodynamics*, Advanced Series on Directions in High Energy Physics, Vol. 5 (World Scientific, Singapore 1989).
- [2] Yu. L. Dokshitzer, V. A. Khoze, A. H. Müller, and S. I. Troyan, *Basics of Perturbative QCD*, Advanced Series on Directions in High Energy Physics, Vol. 5 (Editions Frontieres, Gif-sur-Yvette Cedex, France, 1991)
- [3] J. Gasser and H. Leutwyler, Phys. rep. **87**, 77 (1982); Ann. Phys. **158**, 142 (1984); Nucl. Phys. **B250**, 465 (1985).
- [4] J. Polchinski, Nucl. Phys. **B231**, 269 (1984).
- [5] M. Reuter and C. Wetterich, Preprint HD-THEP-93-40, Heidelberg 1993.
- [6] M. Bonini, M. D’Attanasio, and G. Marchesini, Nucl. Phys. **B409**, 441 (1993).
- [7] U. Ellwanger and C. Wetterich, Preprint HD-THEP-94-1, Heidelberg 1994.
- [8] D. Amati and G. Veneziano, Phys. Lett **B83**, 87 (1979); G. Marchesini, L. Trentadue and G. Veneziano, Nucl. Phys. **B181**, 335 (1981); Ya. I. Azimov, Yu. L. Dokshitzer, V. A. Khoze and S. I. Troyan, Z. Phys. **C27**, 65 (1985).
- [9] Yu. L. Dokshitzer, D. I. Dyakonov, and S. I. Troyan, Phys. Rep. **58**, 269 (1980).
- [10] M. A. Shifman, A. I. Vainshtein, and V. A. Zakharov, Nucl. Phys. **B147**, 448 (1979).
- [11] E. Witten, Nucl. Phys. **B223**, 422, 433 (1983); U. Vogl and W. Weise, Prog. Part. Nucl. Phys. **27**, 195 (1991).
- [12] F. Karsch, Nucl. Phys. (Proc. Suppl.) **B9**, 357 (1989).
- [13] B. Webber, Ann. Rev. Nucl. Part. Sci. **36**, 253 (1986).
- [14] K. Geiger, Preprint CERN-TH. 7409/94, Geneva 1994.
- [15] J. Ellis, Nucl. Phys. **B2**, 478 (1970).
- [16] J. Lanik, Phys. Lett. **B144**, 439 (1984).

- [17] B. A. Campbell, J. Ellis, and K. A. Olive, Phys. Lett. **B235**, 325 (1990); Nucl. Phys. **B345**, 57 (1990).
- [18] M. Shifman, Phys. Rep. **209**, 341 (1991).
- [19] R. Friedberg and T. D. Lee, Phys. Rev. **D15**, 1694 (1977); **D16**, 1096 (1977); **D18**, 2623 (1978); T. D. Lee, *Particle Physics and Introduction to Field Theory* (Harwood Academic Press, New York, 1981).
- [20] L. Wilets, *Nontopological Solitons* (World Scientific, Singapore 1989), and references therein.
- [21] M. Bickeböllner, R. Goldflam and L. Wilets, J. Math. Phys. **D26**, 1810 (1985).
- [22] M. Bickeböllner, M. C. Birse, H. Marshall and L. Wilets, Phys. Rev. **D31**, 2892 (1985);
- [23] G. Fai, R. Perry and L. Wilets, Phys. Lett. **B208**, 1 (1988).
- [24] T. H. R. Skyrme, Nucl. Phys. **31**, 556 (1962).
- [25] V. N. Gribov, Preprint KFKI-1981-66, Budapest (1981); S. D. Bass, Preprint HEP 94/6, Cambridge 1994.
- [26] A. H. Mueller, Phys. Rep. **73**, 237 (1981).
- [27] K. Konishi, A. Ukawa, and G. Veneziano, Nucl. Phys. **B157**, 45 (1979).
- [28] A. H. Mueller and J. Qiu, Nucl. Phys. **B268**, 427 (1986);
- [29] S. J. Brodsky and H. C. Pauly, in the *Proceedings of the 30th Schladming Winter School in Particle Physics*, Schladming, Austria, (1991).
- [30] V. N. Gribov and L. N. Lipatov, Yad. Fiz. **15**, 781 (1972) [Sov. J. Nucl. Phys. **15**, 438 (1972)]; **15**, 1218 (1972) [**15**, 675 (1972)].
- [31] G. Reya, Phys. Rep. **69**, 195 (1981); G. Altarelli, Phys. Rep. **81** (1982).
- [32] J. C. Collins and D. E. Soper, Nucl. Phys. **B194**, 445 (1982).
- [33] A. Bassetto, M. Ciafaloni, and G. Marchesini, Phys. Rep. **100**, 201 (1983).

- [34] L. Durand and W. Putikka, Phys. Rev. **D36**, 2840 (1987).
- [35] J. C. Collins and J. Qiu, Phys. Rev. **D39**, 1398 (1989).
- [36] K. Geiger and B. Müller, Phys. Rev. **D50**, 337 (1994).
- [37] A. Bassetto, M. Ciafaloni, and G. Marchesini, Nucl. Phys. **B163**, 477 (1980).
- [38] F. E. Close, J. Qiu and R. G. Roberts, Phys. Rev. **D 40**, 2820 (1989).
- [39] A numerical solution for inverting Mellin transformed parton distributions is presented in e.g.: R. K. Ellis, Z. Kunszt, and E. M. Levin, Nucl. Phys. **B420**, 517 (1994).
- [40] W. Furmanski, R. Petronzio, and S. Pokorski, Nucl. Phys. **B155**, 253 (1979).
- [41] M. Grabiak and M. Gyulassy, J. Phys. **G17**, 583 (1991).
- [42] E. Eichten, K. Gottfried, T. Kinoshita, K. D. Lane, and T. M. Yan, Phys. Rev. **D21**, 203 (1980); S. R. Gupta, S. F. Radford, and W. W. Repko, Phys. Rev. **D26**, 3305 (1982); P. Moxhay and J. L. Rosner, Phys. Rev. **D28**, 1132 (1983).
- [43] K. Johnson and C. B. Thorn, Phys. Rev. **D13**, 1934 (1976).
- [44] A. H. Mueller, Nucl. Phys. **B415**, 373 (1994).
- [45] J. Kogut and L. Susskind, Phys. Rep. **8**, 75 (1973).
- [46] For the numerical computation, eq. (68) was decomposed into an equivalent system of differential equations which was solved with the program COLSYS, an algorithm for non-linear differential equations.
- [47] K. Geiger and B. Müller, Nucl. Phys. **B369**, 600 (1992); K. Geiger, Phys. Rev. **D47**, 133 (1993); K. Geiger, CERN-TH 7313/94 (1994).
- [48] U. Kalmbach, T. Vetter, T. S. Biró, and U. Mosel, Nucl. Phys. **A563**,584 (1993).
- [49] L. N. Lipatov, Yad. Fiz. **20**, 181 (1974) [Sov. J. Nucl. Phys. **20**, 94 (1975)].
- [50] G. Altarelli and G. Parisi Nucl. Phys. **B126**, 298 (1977).
- [51] D. Amati, R. Petronzio, and G. Veneziano, Nucl. Phys. **B140**, 54 (1978).

FIGURE CAPTIONS

Figure 1: Typical shape of $V(\chi, U)$, eq. (14), with $\partial V/\partial\chi = 0$ at $\chi = \chi_0$ and $V = B$ at $\chi = 0$, where $B = b\chi_0^4/4$ is the bag constant.

Figure 2: Schematics of the parton shower evolution of a fragmenting $q\bar{q}$ pair with its gluon configuration as the virtualities of the partons gradually degrade, starting from the hard scale Q^2 . At large gluon virtualities k^2 the shower develops by perturbative branching processes, but at $k^2 \simeq Q_0^2$ non-perturbative fusion and friction processes set in, such that at $k^2 = \Lambda^2$ no colored fluctuations remain.

Figure 3: Diagrammatic representation of the two-point Greens function of gluons, including both the gluon (self) interactions and the effective interaction with the confining background field χ (indicated by the dashed lines). This gluon propagator describes the evolution of a gluon from a chosen cascade branch in x and k^2 , starting from x_0 and Q^2 .

Figure 4: Diagrams for the interaction probabilities that determine the evolution of the gluon distribution according to (38). In the probabilistic interpretation terms with positive signs lead to a gain of gluons and terms with negative sign to a loss. The gluon with momentum fraction x is the "observed" particle.

Figure 5: The anomalous dimension $\gamma(\omega, k_\perp^2)$ of eq. (44) versus ω for different values of k_\perp^2 .

Figure 6: Comparison between exact expression for the anomalous dimension (44) and the approximations (50) [top] and (51) [bottom].

Figure 7: Behaviour of the distributions $xg(x, k_\perp^2)$ of (56) and (57) for different values of k_\perp^2 . Top part shows result for a flat initial distribution $xg(x, Q^2) = a(1-x)^c$ with $a = 2.8$, $c = 5.3$, and bottom part for a Gaussian initial distribution $xg(x, Q^2) = 1/\sqrt{2\pi c^2} \exp[-(x-d)/(2c^2)]$ with $c = 0.3$, $d = 0.5$. ($Q = 3.5$ GeV, $Q_0 = 1$ GeV, $\Lambda = 0.23$ GeV).

Figure 8: Evolution of the gluon multiplicity $N_g(k_\perp^2)$ from Q^2 down to Λ^2 . At first the gluons multiply, but at $k^2 \approx Q_0^2$ a condensation sets which is complete at Λ^2 ($Q_0 = 1$ GeV, $\Lambda = 0.23$ GeV).

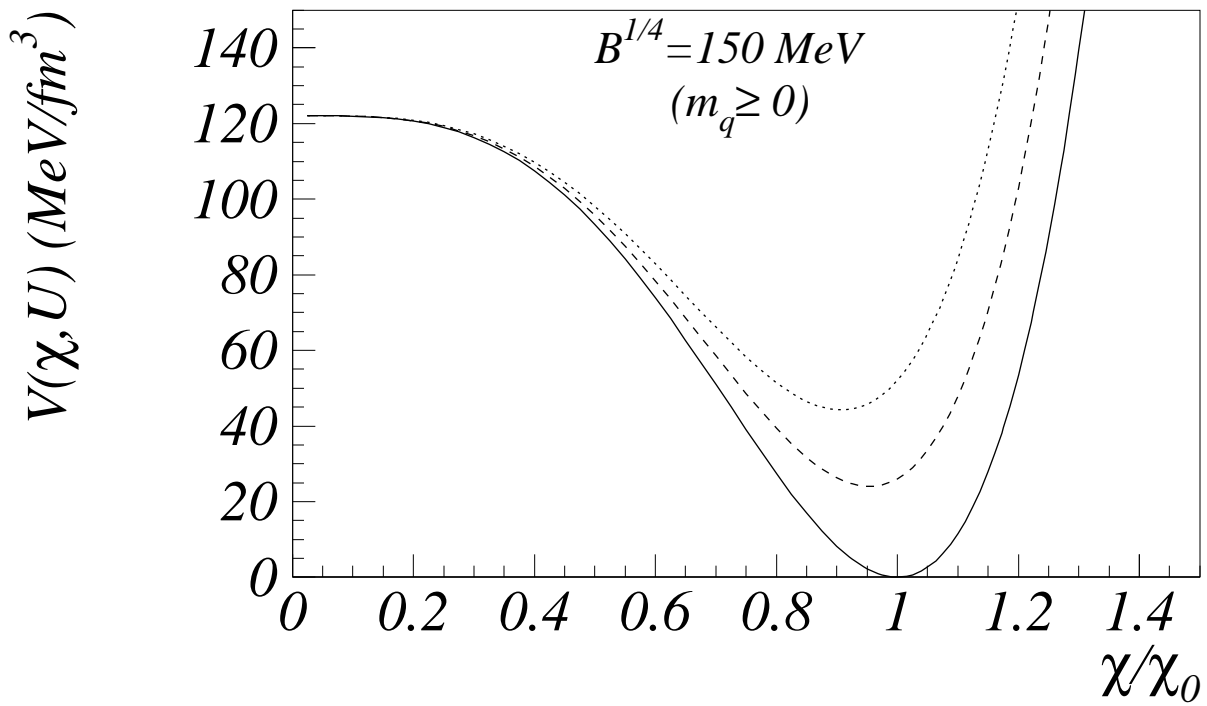
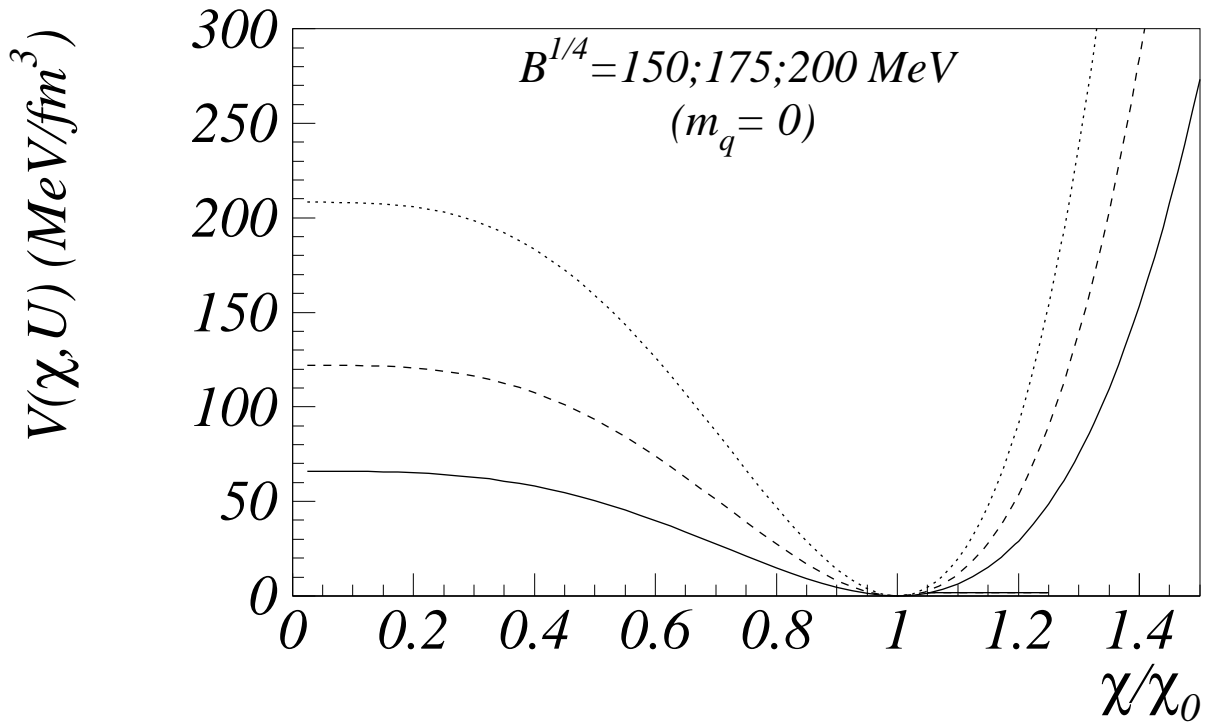
Figure 9: a) String tension t versus separation $R_{q\bar{q}}$ of the $q\bar{q}$ pair, and b) the solutions for χ and κ at $R_{q\bar{q}} = 1$ fm versus r which is the radial coordinate perpendicular to $R_{q\bar{q}}$ ($\chi_0 = f_\pi$ and $B^{1/4} = 150$ MeV).

Figure 10: a) Form of the potential $V[\chi(r)]$ and b) the effective squared mass $M^2[\chi(r)]$ of the χ field, both at $R_{q\bar{q}} = 1$ fm. ($\chi_0 = f_\pi$ and $B^{1/4} = 150$ MeV).

This figure "fig1-1.png" is available in "png" format from:

<http://arxiv.org/ps/hep-ph/9409308v1>

Fig. 1



This figure "fig2-1.png" is available in "png" format from:

<http://arxiv.org/ps/hep-ph/9409308v1>

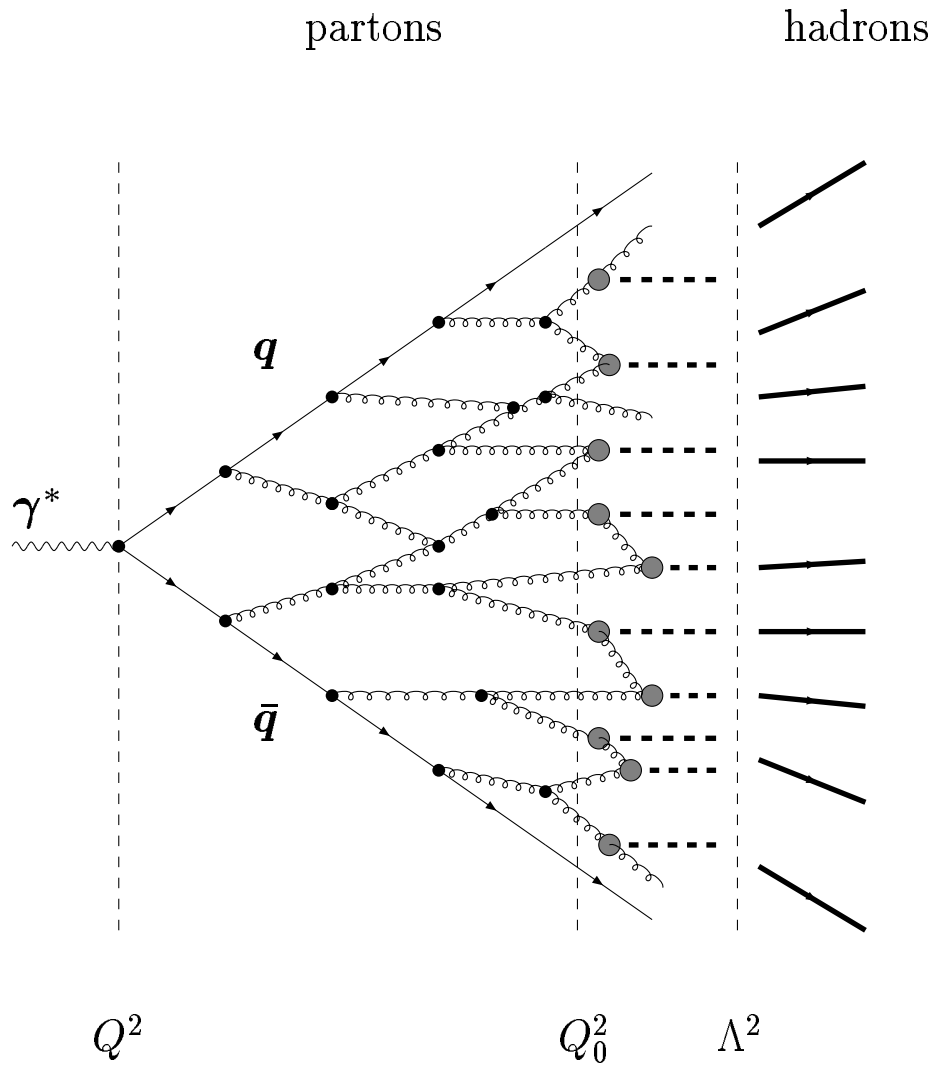
This figure "fig1-2.png" is available in "png" format from:

<http://arxiv.org/ps/hep-ph/9409308v1>

This figure "fig2-2.png" is available in "png" format from:

<http://arxiv.org/ps/hep-ph/9409308v1>

Fig. 2



This figure "fig1-3.png" is available in "png" format from:

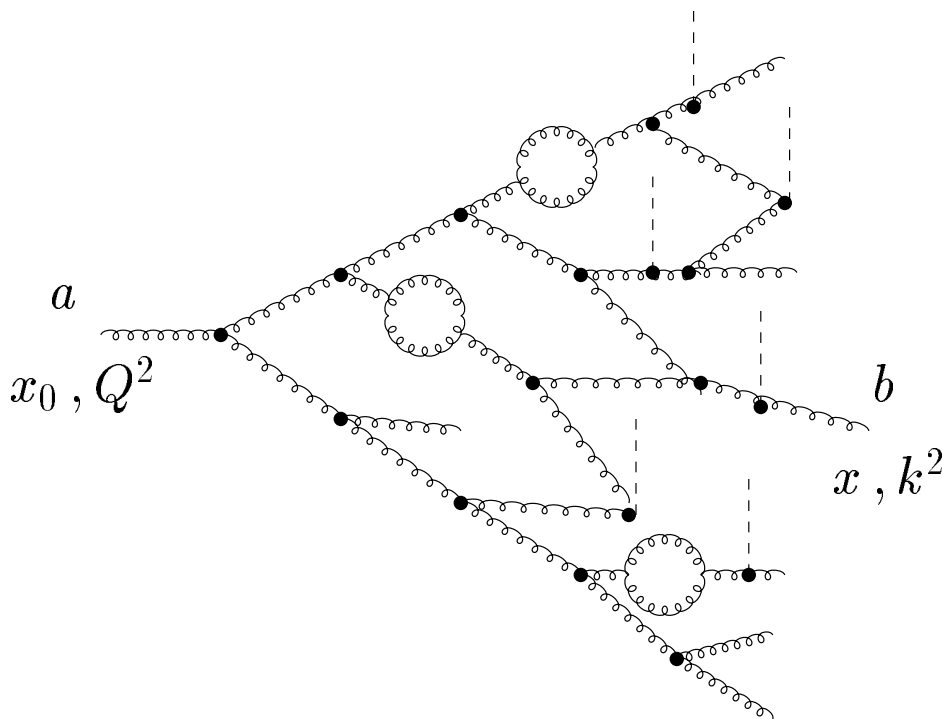
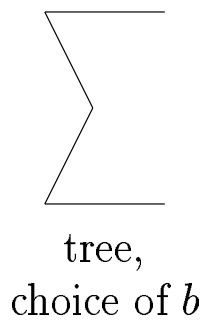
<http://arxiv.org/ps/hep-ph/9409308v1>

This figure "fig2-3.png" is available in "png" format from:

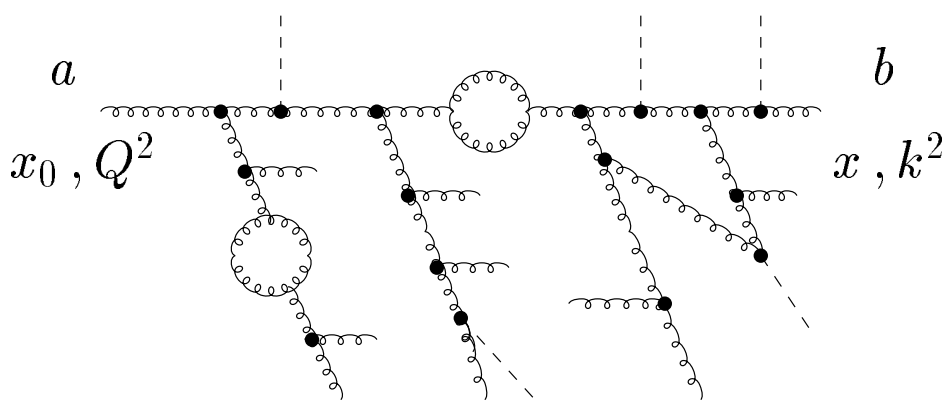
<http://arxiv.org/ps/hep-ph/9409308v1>

Fig. 3

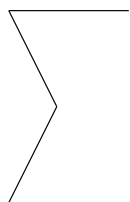
2



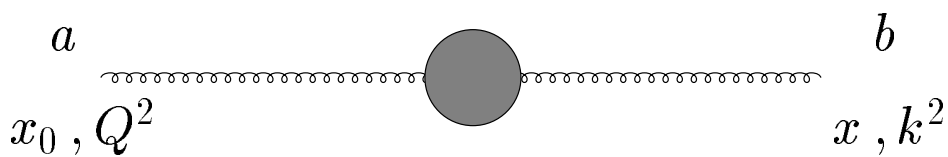
2



=



=



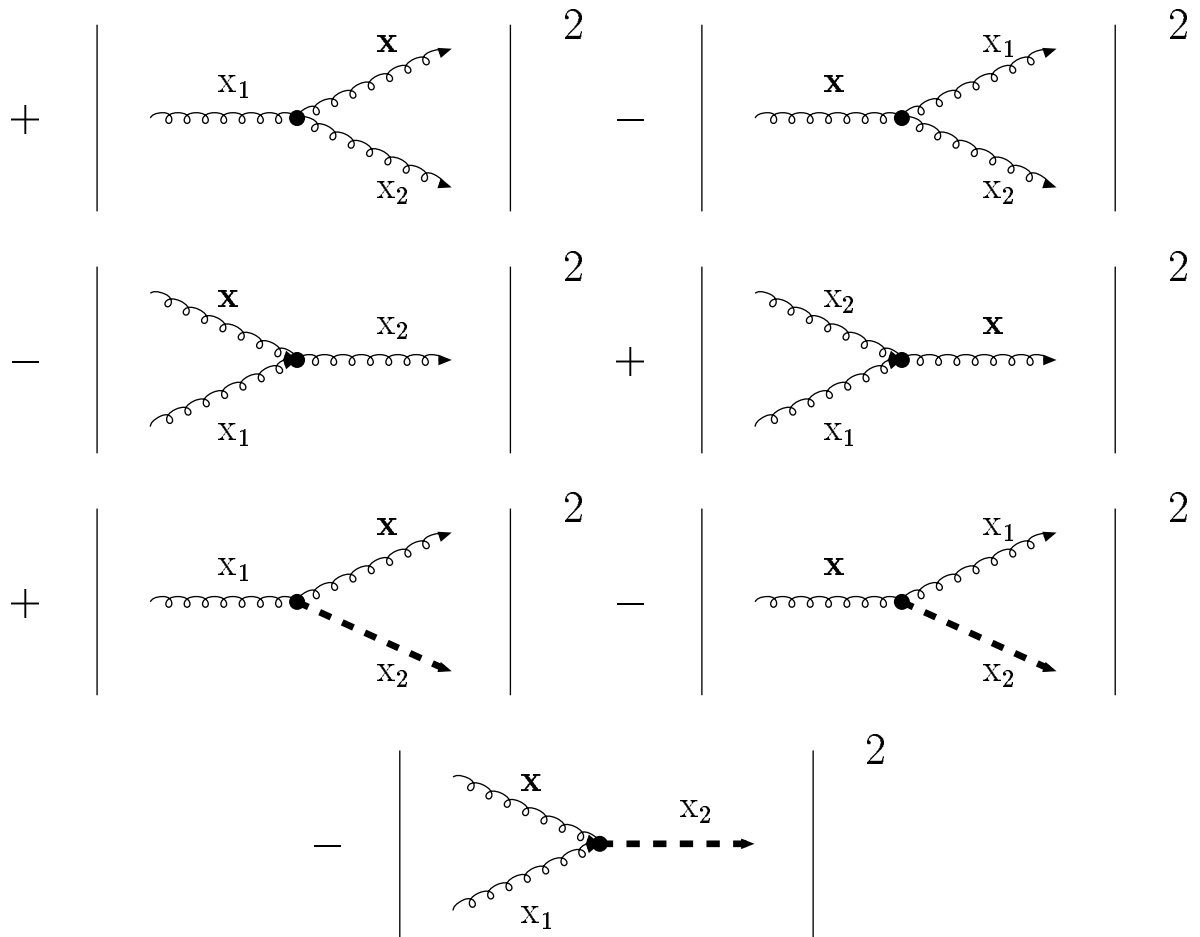
This figure "fig1-4.png" is available in "png" format from:

<http://arxiv.org/ps/hep-ph/9409308v1>

This figure "fig2-4.png" is available in "png" format from:

<http://arxiv.org/ps/hep-ph/9409308v1>

Fig. 4



This figure "fig1-5.png" is available in "png" format from:

<http://arxiv.org/ps/hep-ph/9409308v1>

This figure "fig2-5.png" is available in "png" format from:

<http://arxiv.org/ps/hep-ph/9409308v1>

Fig. 5

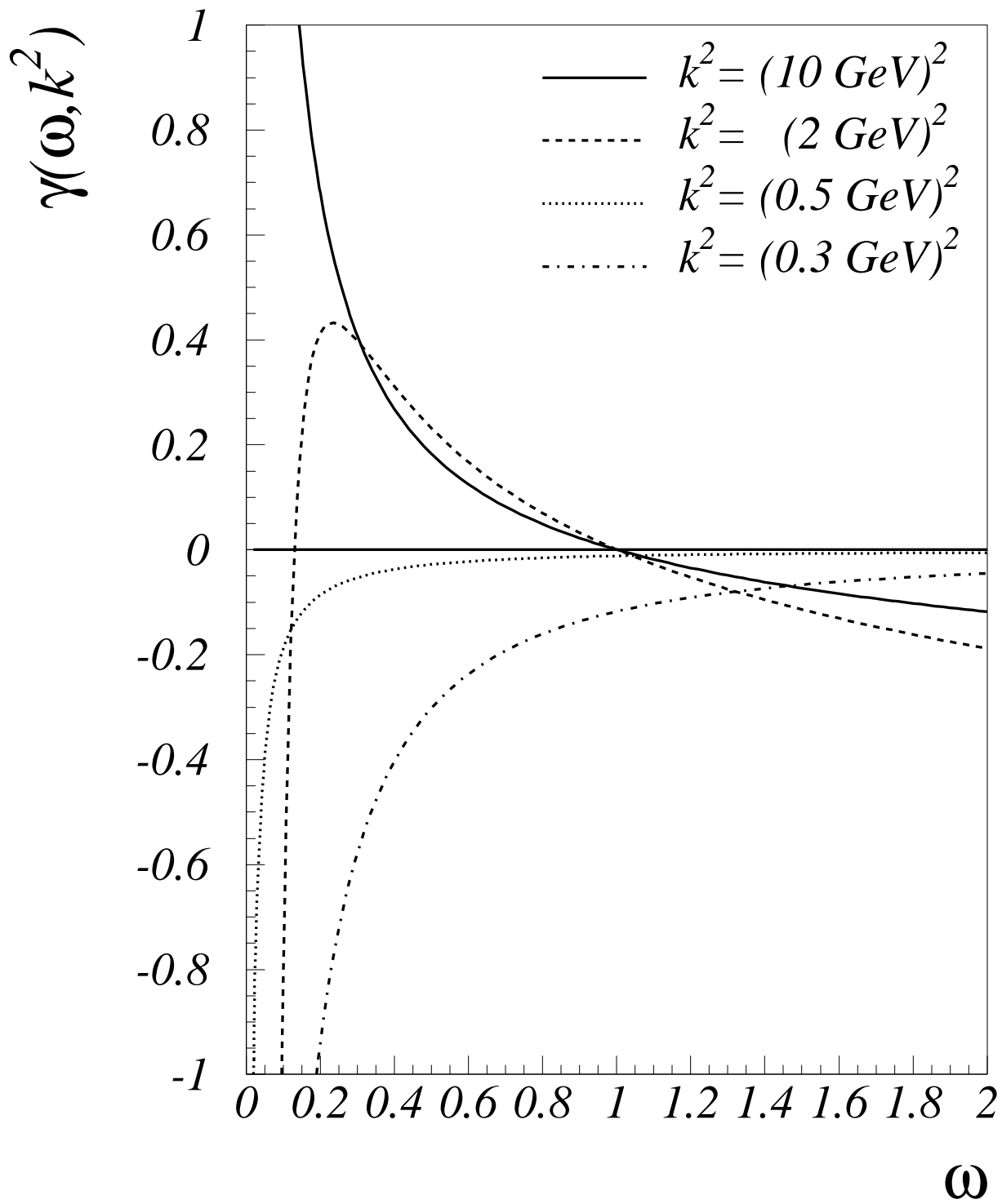


Fig. 6

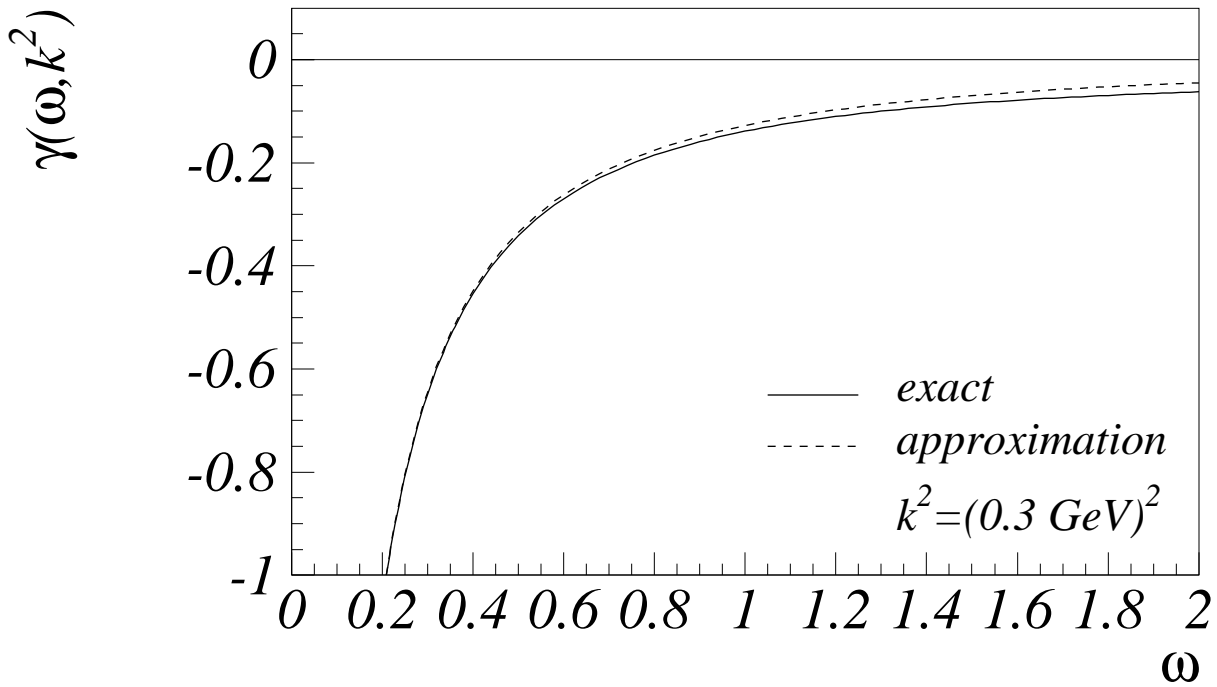
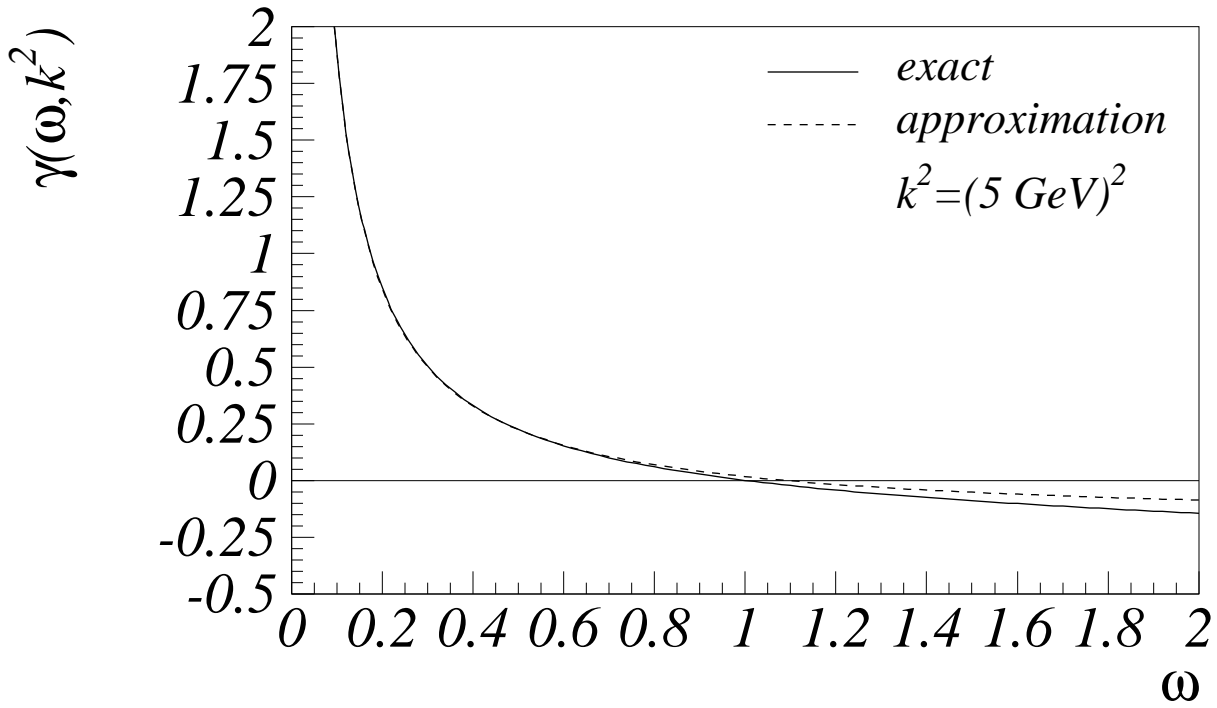


Fig. 7

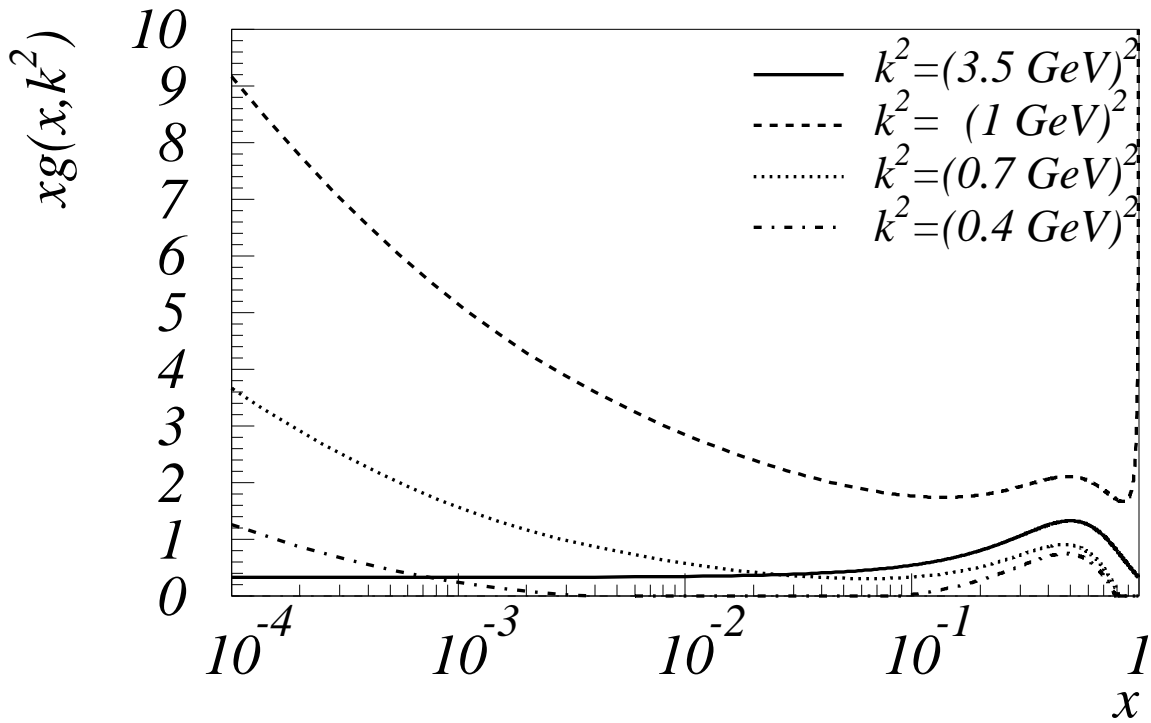
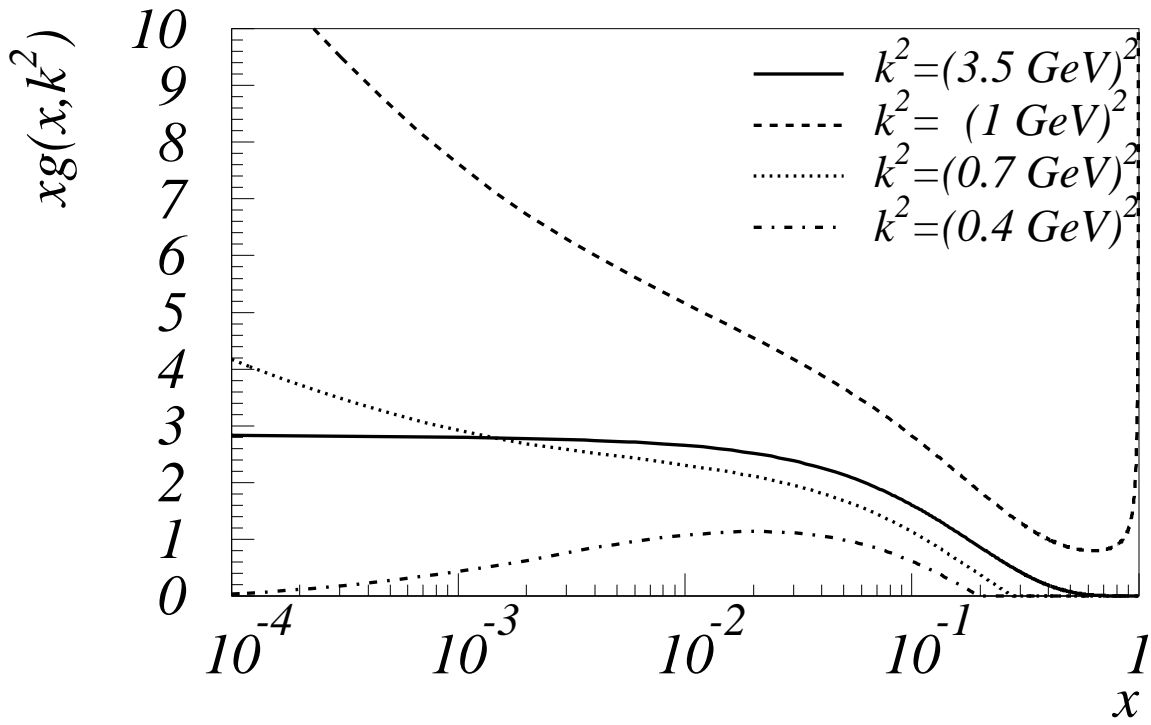


Fig. 8

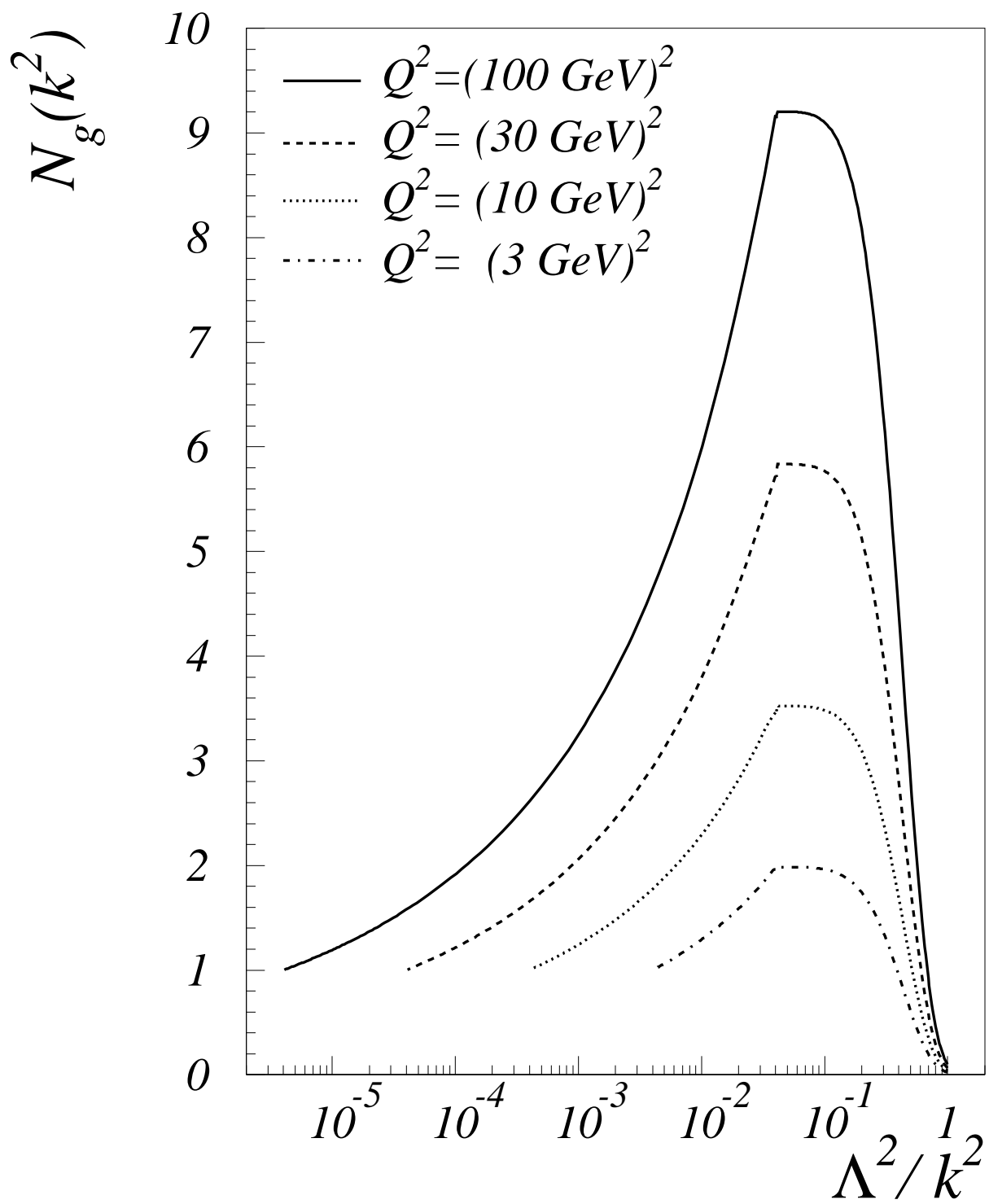


Fig. 9

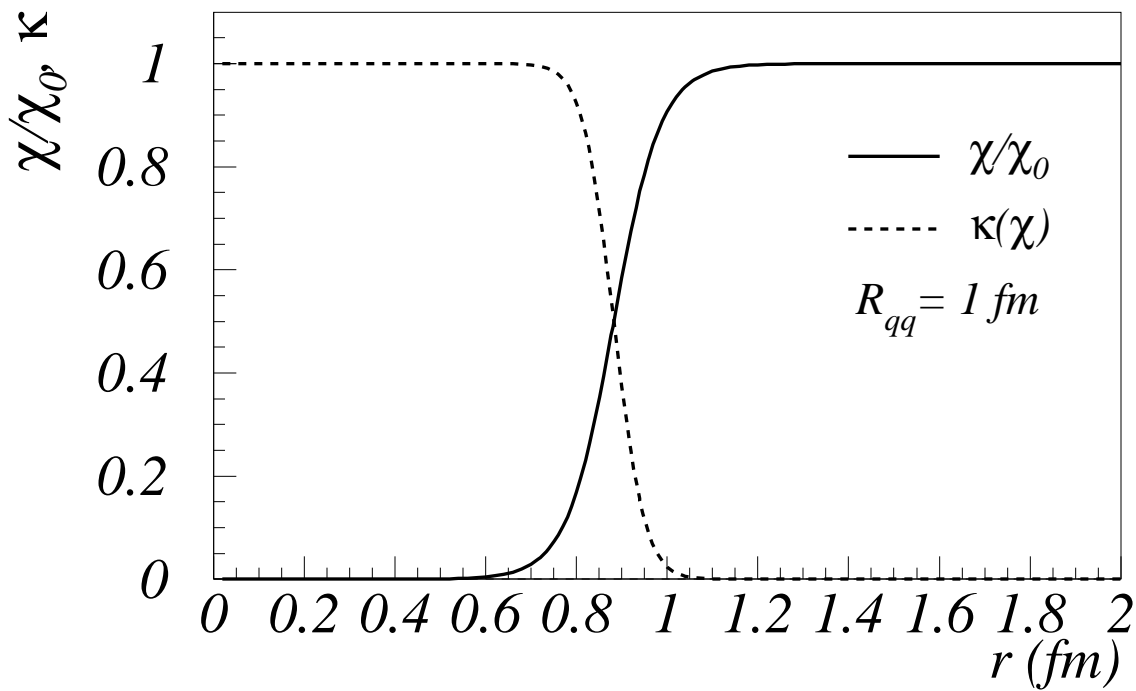
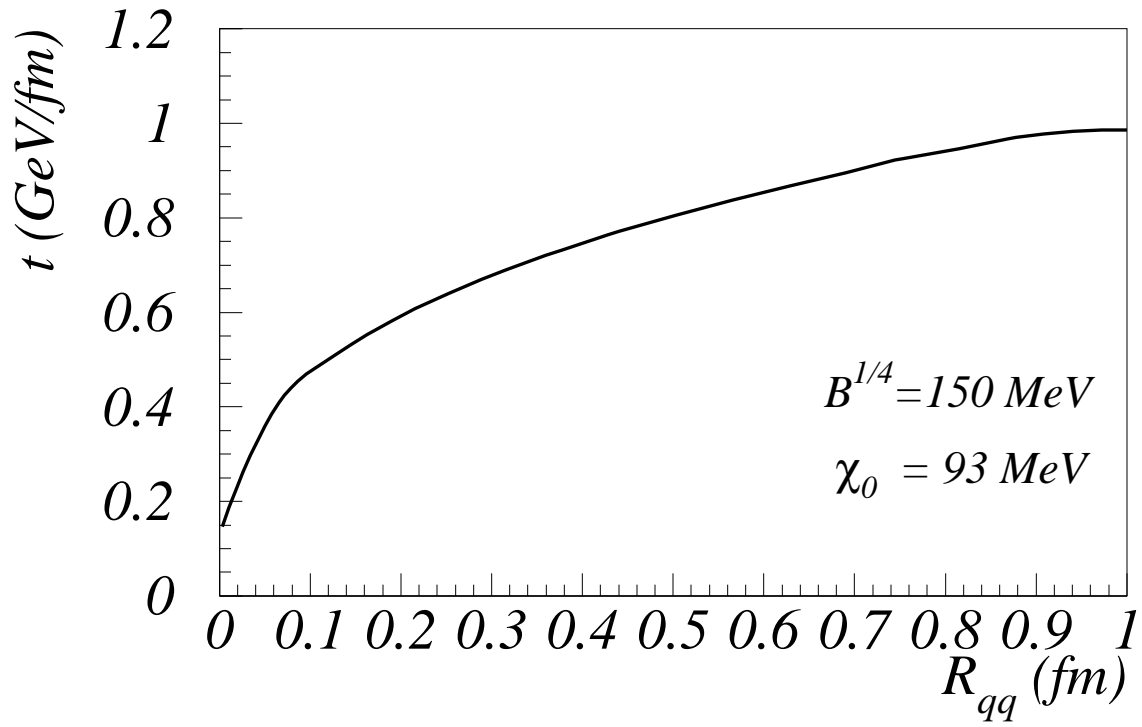


Fig. 10

